UNIVERSITY OF SOUTHAMPTON

Faculty of Physics Sciences and Engineering

Optoelectronics Research Centre

Optical Frequency Comb-locked Signal Generation

by

Win Adiyansyah Indra

Supervisor: Prof. Radan Slavík

Co-Supervisor: Dr. Meng Ding

A thesis for the degree of

Doctor of Philosophy

March 2026

University of Southampton

Abstract

Faculty of Physics Sciences and Engineering

Optoelectronics Research Centre

Doctor of Philosophy

Optical Frequency Comb-locked Signal Generation

by Win Adiyansyah Indra

Supervisor: Prof. Radan Slavík

Co-Supervisor: Dr. Meng Ding

The demand for stable, tunable, and cost-effective laser sources is growing rapidly across applications such as Terahertz signal generation, and precision metrology. This thesis presents the development and characterization of a field deployable, low-cost system for phase-locking telecom-grade tunable lasers to an Optical Frequency Comb (OFC), enabling scalable and high-performance photonic systems.

The research addresses the limitations of conventional OFC-based systems, which typically rely on laboratory-grade lasers, optical amplification, and filtering. Instead, this work demonstrates a compact and field-deployable solution using commercially available tunable lasers and a fully digital feedback loop implemented on a Red Pitaya FPGA platform. A novel PI^4 (proportional–double-integrator) controller architecture was developed to enhance loop bandwidth and suppress phase noise, outperforming traditional PI^2 controllers.

The system achieves stable phase-locking with per-tone OFC powers as low as 1 nW, without the need for optical filtering, making it suitable for multi-laser configurations via passive optical splitting. Experimental results show integrated phase jitter as low as 10 milliradians and long-term frequency stability, measured using Allan deviation, reaching 2×10^{-14} at 1-second averaging time. These experiment setup measurement prove the technique for field deployment by matching or exceeding those of more complicated systems.

Additionally, the thesis examines the system's scalability, showcasing its potential for multi- channel applications and exhibiting steady performance throughout the C-band. Comparative analysis with state-of-the-art THz sources confirms the system’s competitive performance, particularly in terms of tunability and spectral purity.

This work establishes a foundation for accessible, energy-efficient, and scalable OFC-locked laser systems. Future directions include FPGA optimization, multi-laser locking demonstrations, and integration with photonic THz platforms, paving the way for next- generation optical technologies.

Contents

List of Figures

Declaration of Authorship

I declare that this thesis and the work presented in it is my own and has been generated by me as the result of my own original research.

I confirm that:

1. This work was done wholly or mainly while in candidature for a research degree at this University;

2. Where any part of this thesis has previously been submitted for a degree or any other qualification at this University or any other institution, this has been clearly stated;

3. Where I have consulted the published work of others, this is always clearly attributed;

4. Where I have quoted from the work of others, the source is always given. With the exception of such quotations, this thesis is entirely my own work;

5. I have acknowledged all main sources of help;

6. Where the thesis is based on work done by myself jointly with others, I have made clear exactly what was done by others and what I have contributed myself;

7. Parts of this work have been published as: See List of Publications

Signed:..... Date:.....

Acknowledgements

I would like to express my deepest gratitude to all the people who have supported, guided, and inspired me throughout the journey of completing this PhD.

First and foremost, I am profoundly grateful to Prof. Radan Slavík, my supervisor, for his unwavering guidance, encouragement, and exceptional mentorship. His scientific insight, patience, and consistent support have shaped both this research and my development as a researcher. I am equally thankful to my co-supervisor, Dr. Meng Ding, whose expertise, constructive feedback, and continuous motivation have been invaluable throughout this work. I also wish to extend my appreciation to my former co-supervisor, Prof. David Richardson, for his early guidance and for providing the foundation upon which this project was built.

I am especially thankful to my colleagues and collaborators, Dr. Zitong Feng, Dr. Meng Huang, Dr. Xu Hao, Dr. Bo Shi, Irene, and Karim, for their technical help, discussions, friendship, and the many moments that made this journey enjoyable. Their support, whether in the lab or outside it, contributed greatly to the successful completion of this thesis.

My deepest love and appreciation go to my family. To my wife, Jem Tifaokto, thank you for your endless patience, encouragement, and belief in me, especially during the most challenging moments. This achievement is as much yours as it is mine. To my three children, Qarni Aliyana Okwin, Qurrota Muhammad Okwin, and Qaazi Muhammad Okwin, your presence, joy, and innocence have been a constant source of strength and inspiration.

I am eternally grateful to my parents, Abdi Indra and Dinariyati, whose sacrifices, values, and unconditional support have shaped who I am today. I also wish to extend my heartfelt thanks to my parents-in-law, Muruddin Latief and Ona Fithry Zuska, for their continuous encouragement..

And I'd like to thank Indonesian Endowment Fund for Education (LPDP) to support my PhD under Grant 20201022305177.

To all of you, thank you. Without your support, this thesis and this journey would not have been possible.

Definitions and Abbreviations

OFC	Optical Frequency Comb
THz	Terahertz
PID	Proportional–Integral–Derivative
PI	Proportional–Integral
FPGA	Field-Programmable Gate Array
OIL	Optical Injection Lock
PLL	Phase Lock Loop
OPLL	Optical Phase Lock Loop
DWDM	Dense Wavelength Division Multiplexing
ITLA	Integrated Tunable Laser Assembly
DFB	Distributed Feedback
AM	Amplitude Modulation
PM	Phase Modulation
FM	Frequency Modulation
PSD	Power Spectral Density
FDLD	Frequency Delay Line Discriminator
DPD	Digital Phase Detector
RF	Radio Frequency
LNA	Low Noise Amplifier
LPF	Low Pass Filter
VOA	Variable Optical Attenuator
PC	Polarization Controller
OC	Optical Coupler
GPS	Global Positioning System
ADC	Analog-to-Digital Converter
DAC	Digital-to-Analog Converter
SOA	Semiconductor Optical Amplifier
SNR	Signal-to-Noise Ratio
OSA	Optical Spectrum Analyzer
CW	Continuous Wave

List of Publications

Journal Paper

1. **W. Indra**, Z. Feng, M. Ding, J. Vojtěch and R. Slavík, "Tunable Lasers Phaselocked to Optical Frequency Comb," in *Journal of Lightwave Technology*, vol. 43, no. 10, pp. 4833-4839, 15 May15, 2025, doi: 10.1109/JLT.2025.3540298.

2. B. Shi, I.B. Edreira, M. Ding, Z. Feng, **W. Indra**, F. Poletti, G. Marra, and R. Slavik, "Laser stabilized to a fiber interferometer with close-to-zero temperature sensitivity", *Laser & Photonics Reviews*, e02000, 2025, https://doi.org/10.1002/lpor.202502000.

Conference Proceedings

1. **W. Indra**, Z. Feng, J. Vojtěch, M. Ding and R. Slavík, "Phase Locking of a Compact Tuneable Laser to Optical Frequency Comb with Low Frequency Error," *2024 Conference on Lasers and Electro-Optics Pacific Rim (CLEO-PR)*, Incheon, Korea, Republic of, pp. 1-2, 2024, doi: 10.1109/CLEO-PR60912.2024.10676697.

2. **W. Indra**, Z. Feng, J. Vojtěch, M. Ding, B. Shi and R. Slavík, "Towards low-noise tunable THz generation," *2023 International Topical Meeting on Microwave Photonics (MWP)*, Nanjing, China, 2023, pp. 1-2, doi: 10.1109/MWP58203.2023.10416644.

3. **W. Indra**, Z. Feng, J. Vojtěch, B. Shi and R. Slavík, "Tuneable laser locking to Optical Frequency Comb," 2023 Conference on Lasers and Electro-Optics Europe & European Quantum Electronics Conference (CLEO/Europe-EQEC), Munich, Germany, 2023, pp. 1-1, doi: 10.1109/CLEO/Europe-EQEC57999.2023.10232544.

Chapter 1

Introduction

In precision photonics, stabilisation of semiconductor and fiber lasers to highly stable optical frequency references has been an important development. Early approaches relied on locking to narrow-linewidth laboratory lasers or high-finesse optical cavities, which allowed frequency stabilisation at sub-kilohertz levels but often required complicated, environmentally sensitive setups [5], [70]. The invention and rising of OFCs fundamentally transformed this landscape. a dense grid of phase-coherent optical lines with absolute frequencies tracable to microwave or atomic references, OFCs effectively serve as an optical "frequency ruler" [71], [72]. Their introduction allowed direct and routine stabilisation of tunable lasers to absolute or relative optical frequencies with unprecedented accuracy and broad spectral reach [5].

Early demonstrations of comb-referenced locking focused primarily on metrological applications, including optical clock comparisons [69], frequency synthesis [78], and high-resolution spectroscopy [73]–[75]. Analog phase-locked loops with high-speed electronics, high optical powers per comb line, and narrow-linewidth lasers were usually the main components of these systems. Despite their remarkable stability, these methods were frequently restricted to lab settings because of their intricacy, expense, and requirement for optical filtering or amplification in order to isolate distinct comb modes.

In recent times, the focus has switched to deployable and feasible OFC-locked systems that use telecom-grade tunable lasers. Emerging uses like frequency-agile sensing, photonic microwave and THz production [7], and coherent optical communications [6] propelled these developments. Several studies showed that somewhat complex electronics can be used to phase-lock tunable semiconductor lasers to comb lines [8], and advancements in digital phase-locked loop topologies allow for reliable operation even with greater phase-noise sources. However, many implementations still rely on laboratory-grade hardware, require tens to hundreds of nanowatts of per-tone comb power, or depend on tunable optical filters to isolate specific comb modes.

The shift to digital control has made comb-locking methods much more widely available. Although previous systems typically achieved limited lock bandwidths and required higher optical power levels compared to state-of-the-art metrological setups, open and flexible digital PLL platforms [10] and low-cost FPGA-based lockboxes [8] have shown that high-precision optical phase locking can be realized with inexpensive hardware. Parallel progress in OFC technology, such as increased stability, improved spectral coverage, and compact turn-key designs, continues to reduce the barriers to

widespread deployment [85].

All things considered, the previous art clearly shows a path from complicated, high-power, laboratory-grade systems to small, digitally controlled, and power-efficient architectures appropriate for field-deployable and multi-laser applications. Existing demonstrations provide essential foundations but often fall short in scalability, required optical power, or system simplicity, limitations that the present work directly addresses.

1.1 Motivation

Since the first laser concepts were developed, the goal has been to create light emission sources that are as stable and controllable as possible. According to Schawlow and Townes, "a high order of monochromaticity and tunability" would be the most preferred feature. However, they felt that expecting "more than a small fractional amount of tuning in an infrared or optical maser using discrete levels" was unrealistic [1]. This statement was written before the laser diode's discovery [2] [3], which occurred around four years after their comment. The current state of the art is beyond what Schawlow and Townes had considered feasible. In summary, diode lasers can be tuned over a wide spectral range, from far infrared to the ultraviolet, while specific lasers have substantially higher monochromaticity than masers.

The generation of stable and tunable optical signals is fundamental to contemporary photonics, supporting a variety of applications that include high-precision metrology, spectroscopy, advanced telecommunications [4], and the generation of Terahertz signals. As the demand for higher data rates, more precise measurements, and broader spectral coverage continues to grow, so too does the need for laser sources that combine high frequency stability with wide tunability and cost-effective implementation.

OFCs have emerged as a transformative technology in this context. OFCs, which were first developed for frequency metrology, offer a set of equally spaced, phase-coherent optical lines that function as an accurate frequency ruler over a wide spectrum range. This special characteristic has made it possible to make advances in molecular spectroscopy, optical clock creation, and astronomical spectrograph calibration [5]. More recently, OFCs have found increasing utility in non-metrological domains, such as coherent optical communications [6] and photonic generation of microwave and THz signals [7].

Despite their advantages, OFCs are typically used in conjunction with high- performance, laboratory-grade lasers and complex stabilization systems, which limits their accessibility for practical, scalable applications. In many real-world scenarios, such as dense wavelength division multiplexing (DWDM) systems or photonic THz synthesizers, there is a pressing need for multiple laser sources that are not only stable and narrow-linewidth but also tunable and cost-effective. These applications often operate under stringent constraints on size, power consumption, and component cost, requiring low-cost OFC, low-cost tunable lasers, minimum and low-cost optical components, and cheap and low-power consuming electronics for phase locking.

To bridge this gap, recent research [8] has explored the phase-locking of commercially available tunable lasers to OFCs. This method preserves the flexibility and cost-effectiveness of telecom-grade tunable lasers while utilising the OFC's stability. Nevertheless, there are a number of technical difficulties in putting such systems into place. Compared to fixed- frequency lasers, tunable lasers usually have lower intrinsic stability and higher phase noise, and their control bandwidth is often limited [9]. Furthermore, careful system design and optimisation are needed to provide reliable phase-locking from the OFC with minimum optical power, without the need for sophisticated filtering or optical amplification.

Addressing these issues and develop a practical, scalable approach for phase-locking tunable lasers to OFCs are the driving forces behind this study. By doing so, it aims to unlock the potential of OFC-based systems for a broader range of applications, enabling high- performance optical sources that are both accessible and adaptable. The work presented in this thesis paves the way for next-generation photonic systems by showing that high phase stability and tunability can be achieved utilising standard telecom components with careful engineering and inexpensive digital electronics [10] .

1.2 Research Objectives

The primary objective of this research is to develop and characterize a field deployable system for phase-locking telecom-grade tunable lasers to an optical frequency comb. The system aims to meet the following criteria :

- **Low cost and complexity**

  Utilizing commercially available components including integrable tunable laser assemblies (ITLAs) and low-bandwidth digital electronics that widely available, cost- effective, and compact, and no need for laboratory-grade lasers or custom-built sources.

- **Scalability**

  Enabling multiple lasers to be locked to a single OFC through passive optical splitting, avoiding the need for active or tunable component, thereby supporting applications requiring multiple coherent sources.

- **Flexibility**

  Allowing continuous tuning of the locked laser across the C-band.

1.3 Research Contributions

This thesis presents a systematic study of the phase-locking of tunable lasers to an OFC, with several key contributions :

- **Design and Implementation**

  A practical locking system was developed using a Red Pitaya Field Programmable Gate Array (FPGA) platform to implement a digital phase-locked loop (PLL) with a novel PI^4 controller architecture, enhancing loop bandwidth and noise suppression.

- **Performance Optimization**

  The system was optimized to operate with minimal OFC power per tone (as low as 1 nW), eliminating the need for optical amplification or tunable bandpass filters.

- **Comprehensive Characterization**

  Measurements and analyses of both long-term frequency stability and short-term phase noise showed performance metrics that are on par with or better than those of more complicated systems.

- **Scalability Demonstration**

  The feasibility of locking multiple lasers to a single OFC was validated, highlighting the potential for scalable, comb-locked transmitter arrays.

1.4 Thesis Outline

Chapter 2 : Background

Gives an outline of optical locking methods, noise characterisation, OFC, and relevant prior work in the field.

Chapter 3 : Locking Two Tunable Lasers

Describes the experimental setup of phase-locking two ITLA lasers to each other as a performance benchmark.

Chapter 4 : Locking Tunable Laser to an Optical Frequency Comb

Details the implementation and characterization of the OFC-locked laser system.

Chapter 5 : Noise Characterisation

The quality of my locking technique is evaluated in this chapter by measuring the long-term frequency stability, and short-term phase noise of two (2) locked lasers and laser lock to OFC, including comparisons between different controller configurations.

Chapter 6 : Conclusions

A summary of this thesis's main conclusions and some insight into potential future work utilising my phase locking technique will be discussed.

Chapter 2

Background

The previous chapter mentioned the Optical Phase Lock Loop (OPLL) as one of the optical phase lock techniques, along with Optical Frequency Comb (OFC), Tunable Laser, and Noise characterization. This chapter will discuss the background of phase lock loop in optics, the two common techniques for optical phase locking, fundamentals of OFCs, and some of their applications. The second part of this chapter will elaborate on noise characterization of locked lasers, phase noise as a short-term stability measurement and frequency error, and Allan deviation (ADEV) as a long-term stability measurement.

2.1 Optical Phase Locking

Optical phase locking involves getting a laser (the "slave laser") to emit at a frequency that is fixed in relation to another laser's (the "master laser") frequency. By locking lasers to better-quality master lasers, phase locking helps to improve laser quality in terms of frequency and phase noise. This is particularly true for semiconductor lasers, which suffer from frequency and phase noise performance despite being inexpensive. But the technique is not limited to semiconductor lasers, it can be applied to different laser types, depending on system requirements and applications. Two methods of optical phase locking will be covered in this section: optical phase lock loops, and optical injection locking.

2.1.1 Optical Injection Locking

Since the first theoretical and experimental findings on the injection locking of electronic oscillators [11], the concept of synchronising two sources by injection locking has existed. The idea is straightforward, a slave source's laser cavity is filled with a portion of the

output light produced by a master source to achieve locking. The injected signal induces emission inside the slave source cavity, drawing the slave source frequency from its free- running value to that of the master source. The schematic diagram for a general injection locking experiment is displayed in Figure 2.1. below,

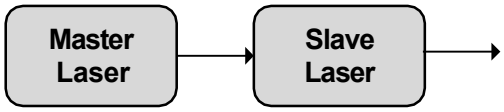

Figure 2.1. Optical Injection Locking, slave laser can be synchronised by injecting the signal from master laser.

The application of the Optical Injection Locking (OIL) theory to laser sources was simple. Injection locking has been proven with various laser types, including CO_2 [12] , XeF [13], and flash lamp pumped dye [14] lasers. One of the earliest semiconductor laser injection locking studies used AlGaAs double heterostructure Fabry-Perot lasers [15], finding that the locking bandwidth depended on the injected power [16]. A theoretical model for injection locking of semiconductor lasers was also provided. Using GaAlAs lasers, the first experiment describing heterodyne injection locking of semiconductor lasers, locking to sidebands as far as 9.5 GHz removed from the fundamental lasing frequency was observed, with low level injection and a locking bandwidth of 400 MHz [17]. Following the publication of the first thorough theoretical investigations of the OIL process of semiconductor lasers [18] [19] [20] [21], the asymmetry of the OIL locking bandwidth was revealed [22]. Additionally, an analysis of instabilities inside the locking range for greater injection levels was published [23], and the development of the Distributed Feedback (DFB) laser injection method began [24]. Later, comprehensive theoretical and experimental studies on DFB [25] [26] [27]and Fabry-Perot
[28] [29] [30] [31] [32] lasers were provided. A parameter quantifying the amplitude-phase coupling in a laser, the effective linewidth enhancement factor, of the injected semiconductor laser could also be measured by using the OIL technique [33] [34] [35] [36]. Since there is no feedback loop and the phase noise suppression achieved by the OIL process only depends on the amount of power fed into the slave laser cavity, it is not subject to the delay time constraints that the Optical Phase Lock Loop (OPLL) process [25]. Therefore, to achieve low levels of phase noise in the OIL system, very small linewidth lasers are not required. However, only a small portion of the locking range is viable due to high level injection's degradation of range stability [29] [32][26].

To sum up, injection locking has shown to be a versatile and effective method for synchronizing laser sources. The method has shown great promise from early experiments with different kinds of lasers to more sophisticated theoretical and experimental studies on semiconductor lasers. Particular benefits of the OIL process include phase noise suppression without the use of feedback loops. However, the stability of the locking range can be compromised at high injection levels. Overall, injection locking is still a useful technique for creating accurate and reliable laser systems.

The OIL technique is limited by injection ratio and linewidth enhancement factor though, narrow locking range at low injection power. In practical systems, the random drifts of temperature and laser bias currents can easily cause master-slave frequency detuning $\Delta\omega$ drifts outside the locking range $\Delta\omega_{LR}$, causing unlocking of the OIL laser. Thus, the frequency offset needs to be controlled. Fine control of $\Delta\omega$ is particularly important for applications requiring low injection ratio because of the small locking range [9] .

2.1.2 Optical Phase Lock Loop

OPLL is a feedback mechanism that controls the optical phase of an optical source by tracking the optical phase excursions of an incoming optical signal. This is accomplished by creating a phase error signal that controls the local source frequency by comparing the input signal's phase to that of the local optical source. The input signal source is known as the master source, and the local source is known as the slave source. An OPLL's general schematic diagram is shown in Figure 2.2.

The frequencies at which master and slave sources function varies in heterodyne systems. The master and slave laser outputs are combined on a photodetector, resulting in a beat signal at the output that matches the offset frequency between the two sources. The beat signal's phase is compared to that of an offset synthesizer operating at a frequency that is similar to the beat signal. The output of the phase detector then produces a phase error signal. The loop filter modifies the slave laser after processing this signal in order to reduce phase inaccuracy. When the frequency offset between the two optical sources remains constant and matches that of the offset synthesizer , the loop gains locks.

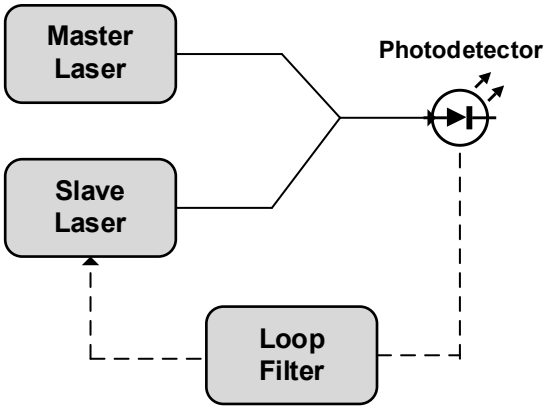

Figure 2.2. Schematic of OPLL in homodyne configuration.

In the past, a number of technical issues have restricted the use of OPLL systems. The availability of optical sources was one of them, and possibly the most significant. The most used optical sources were lasers, which have poor frequency tuning response, frequency instability, and wideband phase noise. The OPLL is a potential method for laser synchronization since the development of semiconductor lasers, which offered small and easily adjustable sources. In order to receive radio signals in Amplitude Modulation (AM) coherently, the concept of phase locked loop to synchronize two sources was initially presented in 1932 [37] . Phase-lock methods have been in use ever since. Examples include the synchronization of television receivers [38], the control of phased array antennas [39], the coherent creation of phase and frequency modulated signals [40], and the stabilization of microwave oscillators [41]. A homodyne system with 633 nm HeNe lasers [42] and a slave source adjusted by a piezoelectrically positioned mirror was among the first OPLLs to be published. The interference pattern rings at the OPLL output, which came after the beam splitter that combined the laser outputs, were used to observe the locking condition.

Following that, numerous other works were created utilizing various laser types and frequency tuning procedures. CO_2 lasers [43] operating at 10.6 μm and modulated by an internal electro-optic frequency modulator and a piezoelectrically positioned mirror were used to realize a homodyne system. HeNe lasers were also used to create heterodyne systems, which produced signals at 2 MHz [44] and 5 MHz [45]. More recently, homodyne
[46] [47] and heterodyne OPLLs that produce 4 GHz [48] and 12 GHz [49] modulated signals have made use of solid state lasers. Low phase noise lasers with a very narrow linewidth (less than 200 kHz) were employed in every instance. Since any frequency correction may be
accomplished directly through the laser bias current, using semiconductor lasers would guarantee quick and ease tuning.

However, these sources could not be used in OPLL systems due to the quantity of phase

noise they presented. Weakly linked exterior cavities were utilized to reduce the system semiconductor laser linewidths in a heterodyne OPLL, one of the earliest experiments employing semiconductor lasers [50]. The use of two distinct laser types in homodyne OPLL configurations has also been suggested as a way to reduce the complexity of the OPLL system. In these designs, a HeNe laser input signal is locked to an external cavity semiconductor laser that is adjusted by a $LiNbO_3$ modulator [51]. Improved external cavity semiconductor lasers were employed in both homodyne OPLLs [52] and heterodyne OPLLs [53]. The semiconductor laser linewidth could also be reduced by using optical feedback from external high-finesse resonators. This method was applied to homodyne OPLLs [54] and heterodyne OPLLs, producing signals at 25 MHz [55] and 40 MHz [56].

The potential for rigid, compact, and affordable systems is the benefit of employing semiconductor lasers without line narrowing techniques. Narrower linewidth lasers are now achievable thanks to advancements in semiconductor laser structures or materials. The first loops employing semiconductor lasers without line narrowing were documented. Double quantum well lasers [57], three electrode DFB [58], and extended cavity semiconductor lasers
[59] were used to create heterodyne systems. These loops could provide good system phase noise performances (phase error variances of 1 rad^2, 0.04 rad^2, and 0.004 rad^2, respectively), but they could not be used with better loop filter setups. It was determined that the laser linewidth, loop gain, and bandwidth requirements for realistic loop propagation delay values were the main issues with implementing OPLLs with non-line-narrowed semiconductor lasers. The loop delay restricts the system's phase noise reduction by limiting the loop gain and bandwidth. The poor phase noise suppression necessitates a low laser linewidth (less than a few MHz) to offer adequate loop performance unless sophisticated loop electronics [57] or passive loop filters [58] are constructed, methods that can ensure short loop delay.

Overall, OPLLs are essential for tracking and resolving phase faults, which helps to synchronize optical sources. The performance of OPLLS has been dramatically enhanced by developments in semiconductor laser technology despite early issues with phase noise and frequency instability in lasers. Contemporary OPLLs' ability to produce high-frequency optical signals with minimal phase noise makes them useful for a range of applications. However, loop delay and phase noise suppression requirements continue to be obstacles to using OPLLs with non-line-narrowed semiconductor lasers.

2.2 Noise Characterisation

An ideal sinusoidal wave is represent by,

$$E(t) = E_o \cos (\omega_o t + \theta_o), \quad (1)$$

where t is time, $E(t)$ is the electric field, E_o is the amplitude, ω_o is the angular frequency, and θ_o is the initial phase.

Unfortunately, there are no perfect signals in the actual world. Noise will always be present in the signal's amplitude portion as well as in its phase. Figure 2.3. shows the displacement from an ideal sinusoidal wave, random changes in amplitude and/or phase that weaken the signal of interest are referred to as amplitude noise and phase noise, or regarded as oscillator noise. A laser's frequency fluctuates due to several processes, which also contribute to its noise. These are usually environmental changes like temperature, vibrations, and humidity or air pressure. Additional sources may include noise in the laser's temperature control or current driver. Later in this dissertation, noise sources will be covered in greater detail. An electrical or optical signal that is noisy can be explained by,

$$E(t) = [E_o + \alpha(t)] \cos [\omega_o t + \theta_o + \theta(t)] \quad (2)$$

where $\alpha(t)$ is the amplitude noise and $\theta(t)$ is the phase noise.

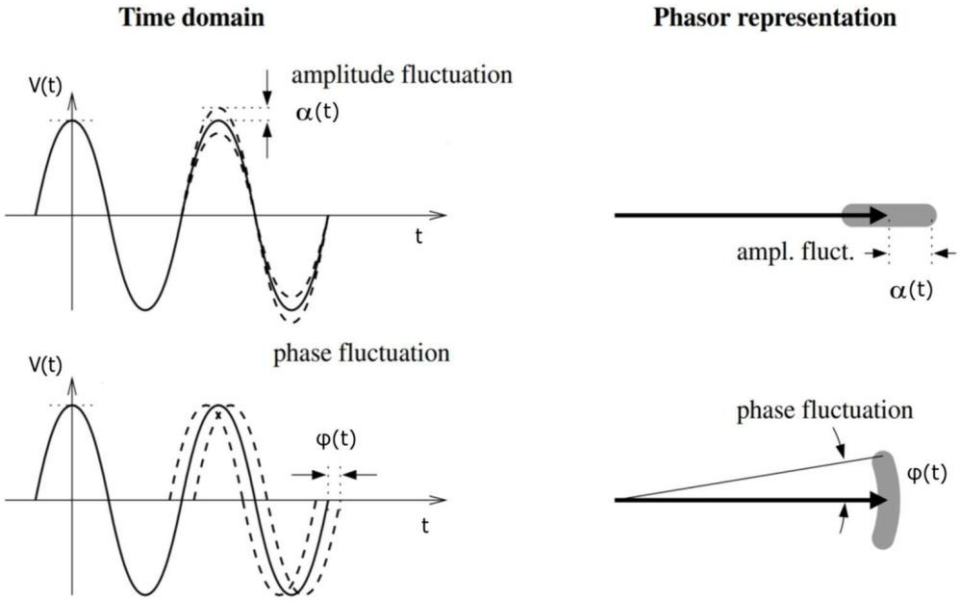

Figure 2.3. Amplitude noise and phase noise. Adapted from [60].

2.2.1 Phase Noise

In the equation (2), $\theta(t)$ is the second extra term. The phase noise is represented mathematically by this quantity. Anything that causes $\theta(t)$ to be nonzero is considered noise. The oscillating sinusoid exhibits phase modulation due to a nonzero $\theta(t)$ term. The introduction of modulation sidebands around the fundamental frequency is the result of phase noise modulation. In general, phase and amplitude noise may be the cause of the modulation sidebands. However, by using a digital phase detector in our experiment, the amplitude noise may be removed. The detector is insensitive to amplitude variations as long as the signal is strong enough to be detected, meaning amplitude noise is not directly passed into the phase error signal.

Transistors, resistors, capacitors, inductors, and crystals are some of the parts used to make oscillators. These elements are not all perfect. Environmental influences can have an impact on the oscillator's components and, consequently, its output. Temperature, pressure, gravity, dust buildup, and voltage stress can all alter an oscillator's output. Moreover, some components only undergo a gradual change in their properties. The noise sources listed above usually happen gradually and over an extended length of time. Long-term stability is the term used for this. Other noises come in short spurts and at random. We refer to this as short-term stability. In general, noise that happens over extremely short time scales is referred to as phase noise. Up to high frequencies >> 1 Hz, phase noise measurements are often shown in the frequency domain. Short-term noise can lead to difficult-to-detect faults and issues in systems. For instance, a mechanical shock could produce temporary noise. Errors can also be introduced into electrical systems by disturbances on power lines. Lastly, short-term noise is typically the more problematic because long-term noise is simpler to detect and correct. The limiting factor in microwave and radio frequency systems is usually phase noise. Frequency stability is directly correlated with phase noise. In addition, phase noise in electrical systems can cause errors and decreased performance. A weak intended signal may be obscured by phase noise sidebands, making processing the signal challenging or impossible. Phase noise has the potential to raise the bit error rate in digital communication systems. Lastly, radar systems may experience issues due to phase noise. The weak desired Doppler signal in coherent Doppler radar may get cluttered by phase noise sidebands created by a strong interfering signal caused by reflections from big stationary objects [61].

Phase noise can only be evaluated when a reference signal that is significantly quieter (lower phase noise) than the signal under test is available, ensuring that the measurement reflects the noise of the device being characterized rather than the reference [62]. This makes it possible to assume that the reference signal's noise contributes very little to the measurement. The reference signal's

frequency should be set so an RF spectrum analyzer and a sufficiently quick photodetector can measure the beating with the test signal. Phase noise can be measured using a variety of methods, each with pros and cons. Direct spectrum analyzer testing, is the simplest measurement method. In this approach, the device under test is connected directly to the spectrum analyzer, and the signal spectrum is recorded. . Figure 2.4 shows example of phase noise measured. When performing a phase noise measurement using a spectrum analyzer, it's crucial for the user to recognize that the system doesn't solely measure phase noise. The spectrum analyzer depicts the combined signal power observed by its filter across different frequencies. This signal comprises both amplitude and phase noise, and the displayed result represents the sum of both types of noise. The spectrum analyzer lacks the ability to differentiate between the two. While there may be instances where amplitude noise exceeds phase noise at specific frequency offsets, this is not the typical scenario and is generally limited in range.

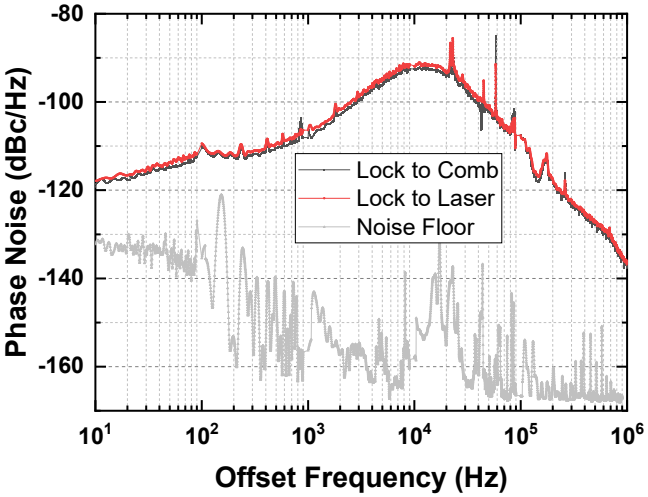

Figure 2.4. Spectrum of phase noise measured.

A self-referenced heterodyne approach can measure the phase noise in situations where a higher-quality reference is unavailable [63]. In this instance, the signal is divided into two arms, one of which is frequency-shifted and delayed about the other. The delay must be greater than the signal's coherence length for the two signals to be de-correlated upon recombining. Each arm will contribute equally to the observed phase noise if the noise is stationary. By merely measuring the Power Spectral Density (PSD) of the beat signal, the phase noise spectrum may be determined. When the data are displayed, the PSD is often normalized to the RF carrier power (the beat signal's core frequency). The resulting spectrum, which is expressed in dBc/Hz (decibels concerning the carrier per Hz), displays the sideband power caused by noise relative to the carrier. The primary drawback of this measurement is that because both types of noise produce sidebands, the PSD of the beat signal cannot discriminate between amplitude and phase noise. Additionally, the beat signal's frequency

must be extremely constant to do this measurement and not fluctuate compared to the spectrum analyzer's sweep time.

Another technique to measure phase noise is Frequency Delay Line Discriminator (FDLD) Technique, as shown in Figure 2.5. The FDLD method is a classical analog technique used to convert phase fluctuations into voltage fluctuations by exploiting the time delay between two signal paths. It is particularly useful for measuring phase noise in free-running oscillators or lasers. The basic principle is that the signal is split into two paths: one path is delayed by a known time τ (typically using a long coaxial cable or an optical fiber), while the other path remains undelayed. . The two signals are then recombined in a mixer or phase detector. The output voltage is proportional to the differential phase between the two paths. The discriminator's sensitivity is directly proportional to the delay τ. Short delays result in poorsensitivity to low- frequency phase noise. Long delays improve sensitivity but introduce Increased insertion loss and higher susceptibility to environmental noise (e.g., temperature drift, mechanical vibrations). It's because the phase noise of a laser is a time-dependent fluctuation, the shorter the delay, the less time the laser has to accumulate phase error. It means the phase difference between the two paths becomes less pronounced, making it difficult to detect small fluctuations. And Vice versa, longer delay means it will be easier to detect small fluctuations.

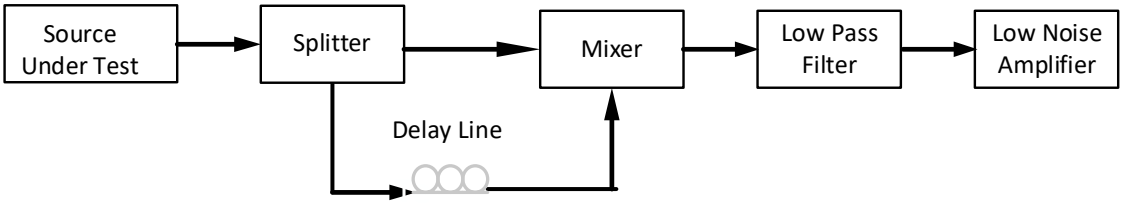

Figure 2.5. Block diagram of a frequency delay line discriminator phase noise measurement system.

In the setup, the delay line may not have been long enough to resolve the low-frequency phase noise components of interest (e.g., <1 kHz), or it may have introduced excessive noise. Achieving accurate phase noise measurements requires precise knowledge of both the delay τ and the system's transfer function. Any mismatch in cable lengths, impedance, or phase imbalance can distort the measurement. And without proper calibration, the output spectrum may not accurately reflect the true phase noise. The FDLD technique is inherently linear only for small phase deviations. If the phase fluctuations are large (e.g., during lock acquisition or under environmental perturbations), the system may operate in a nonlinear regime, distorting the output. The analog components (mixers, amplifiers, delay lines) contribute their own noise. The noise floor of the FDLD setup may have been too high to resolve the ultra-low phase noise levels achieved in your OFC-locked system (e.g., <–120 dBc/Hz). This would result in a flat or noisy spectrum that masks the actual performance.

As an alternative, there is Digital Phase Detector (DPD) as a technique to characterize phase noise as shown in Figure 2.6.

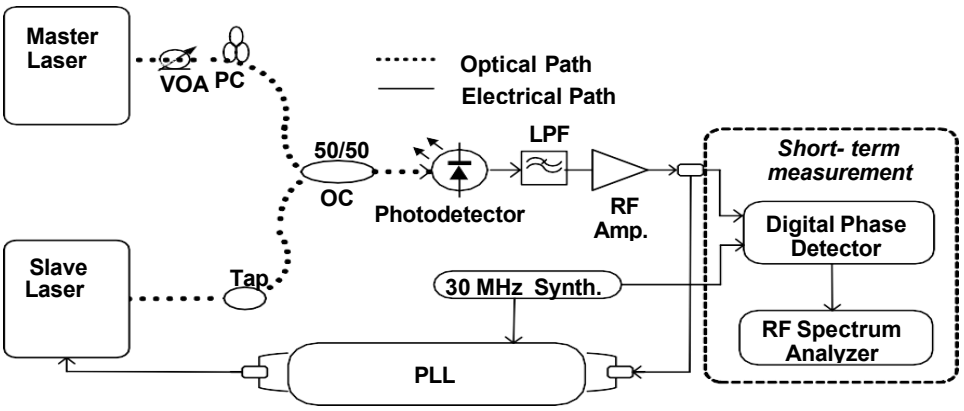

Figure 2.6. Schematic for measuring the phase noise of a laser using Digital Phase Detector (DPD).

A DPD takes two input signals, a reference signal and beating signal from two lasers locked (Master laser and Slave laser). DPD will compare the phase difference between these signals and generate an output signal that is proportional to this phase difference. The DPD operates by utilizing a digital logic gate, as the central component of the circuit. The simple one is XOR gate. The gate generates a high output when the input signals are out of phase, and a low output when they are in phase. Unlike analog phase detectors, DPDs detect signal edges rather than amplitude levels, making them less susceptible to amplitude noise and variations. They find widespread use in applications such as frequency synthesizers, phase-locked loops, and other scenarios that demand precise phase detection [64].

To sum up, one important aspect influencing oscillators' stability and performance is phase noise. It comes from a variety of sources, such as component flaws and ambient influences, and it can cause serious problems in microwave and radio frequency systems. Phase noise must be precisely measured, and one technique to lessen amplitude noise is to use a digital phase detector (DPD). Understanding and being able to control phase noise are essential for improving the reliability and performance of electronic systems.

2.2.2 Allan Deviation – frequency stability

As mentioned previously, long-term stability is affected by noise stemming from environmental influences like temperature, pressure, gravity, and dust buildup. These factors can alter an oscillator's output gradually over an extended length of time, generally corresponding to long sampling times >> 1 s, which correspond to frequencies << 1 Hz. The schematic for measuring

long-term stability is shown in Figure 2.7.

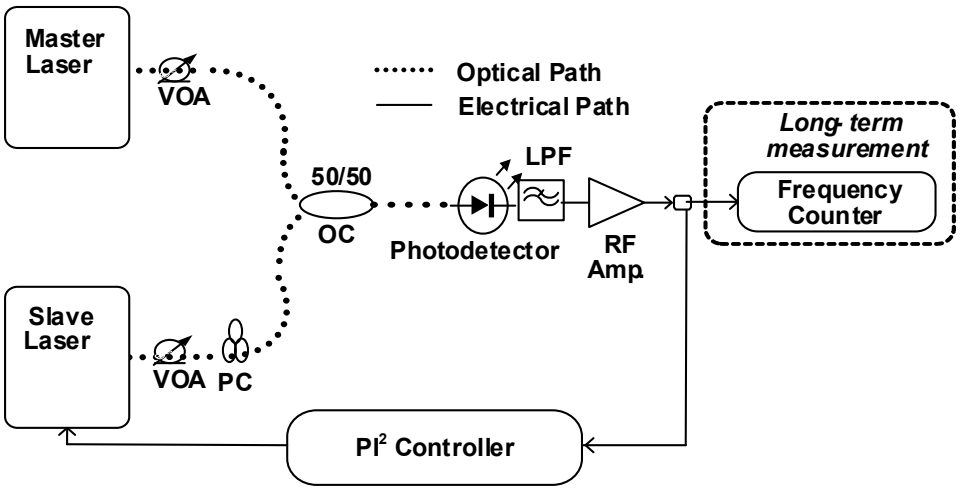

Figure 2.7. Schematic for measuring long-term stability using frequency counter.

An RF frequency counter, which counts the amount a signal crosses zero over a predetermined period of time (the gate time), can be used to precisely measure the beat signal's frequency. When a highly stable signal is used as the reference (master), it is possible to determine the frequency stability of a test signal by repeatedly tracking frequency variations with a frequency counter. Statistical variance can then be calculated in order to describe the frequency stability. Although the standard deviation is frequently employed as a generic tool to assess the dispersion of a data collection, it is unsuitable to explain frequency stability. This is because the standard deviation for many frequency sources, which is calculated based on the mean of the entire data set, is not stationary and will vary depending on the number of samples in the data set [65]. This is due to the presence of noise which is correlated with time (non-white noise), e.g. 1/f flicker of phase noise. The Allan deviation, $\sigma^2(r)$, has become a common method for measuring frequency stability in the metrology community. The Allan variance formula, $\sigma_y^2(r)$, is given by,

$$\sigma_y^2(r) = \frac{1}{2(N-1)} \sum_{i=1}^{N-1} (y_{i+1} - y_i)^2 \qquad (3)$$

where y_i is the fractional frequency measured over a sampling time of r, with the subscript i referring to the i^{th} measurement out of N number of measurements.

The Allan deviation is a statistical indicator of the frequency stability of a clock or oscillator that offers a more precise and insightful description of the oscillator's stability than the standard deviation. The fact that the Allan deviation takes into account the kind of noise that is present in the system being monitored is one of its key advantages over the standard deviation. The Allan deviation, in particular, is intended to assess the stability of the system's frequency, which is

impacted by many noise sources, including flicker noise, white noise, and random walk noise, as shown in figure 2.8.

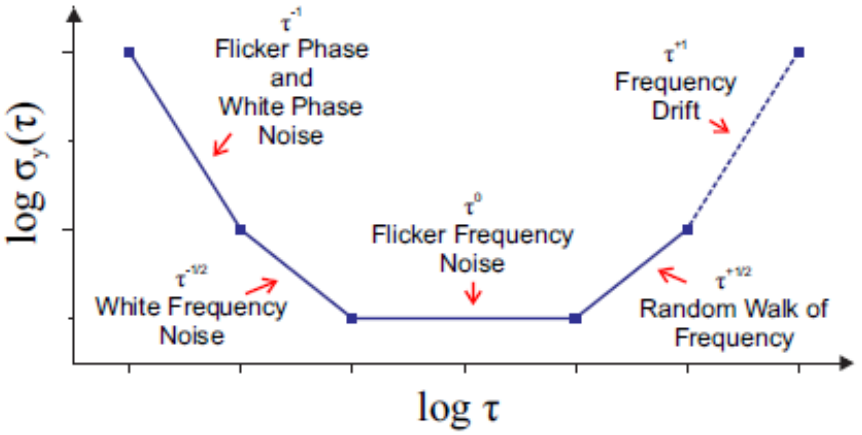

Figure 2.8. Allan Deviation plot with the different types of noise sources [60].

Random walk FM noise usually relates to the Oscillator's Physical Environment. If random walk FM is a predominant feature of the spectral density plot then Mechanical Shock, Vibration, Temperature, or other environmental effects may be causing "random" shifts in the frequency carrier. Flicker FM a noise may typically be related to the Physical Resonance Mechanism of an active oscillator. Flicker FM is common in high-quality oscillators, but may be masked by white FM or flicker PM in lower-quality oscillators. White FM noise is a common type found in passive-resonator frequency standard. These contain a slave oscillator, often quartz, which is locked to a resonance feature of another device which behaves much like a high-Q filter. Cesium and rubidium standards have white FM noise characteristics. Flicker PM noise may relate to a physical resonance mechanism in an oscillator, but it usually is added by noisy electronics. This type of noise is common, even in the highest quality oscillators, because in order to bring the signal amplitude up to a usable level, amplifiers are used after the signal source. Flicker PM noise may be introduced in these stages. It may also be introduced in a frequency multiplier. White PM noise is broadband phase noise and has little to do with the resonance mechanism. It is probably produced by similar phenomena as flicker PM noise. Stages of amplification are usually responsible for white PM noise [66] .

By using Allan deviation to measure the frequency stability of a source, the requirements are depend on the application. Each appplication generally has its own value of Allan deviation stability. The frequency instability of 4.4×10^{-15} at averaging time 1s for 0.66-Terahertz signal, generated by photomixing a pair of comb lines extracted coherently from the source comb [67]. The noise analysis of different sensor types using Allan deviation. Compared to the conventional variance that assesses the variation around the mean value of the aggregate data surveyed, Allan deviation estimates variations by averaging measurements for different periods [68].

To summarize, the long-term stability of oscillators is influenced by environmental factors, which cause gradual changes over time. An RF frequency counter is used to measure this stability, and statistical variances such as Allan deviation, which gives a more precise picture of frequency stability than standard deviation are computed. Understanding and mitigating different types of noise, such as flicker noise and white noise, is crucial for maintaining oscillator performance across various applications.

2.3 Optical Frequency Combs (OFC)

Although phase locking is the main focus of this thesis, as discussed in the beginning of this chapter, it is equally critical to comprehend the original laser being "copied." The master laser is the name given to this laser. The master laser used in this thesis will be an OFC. An OFC, as shown in figure 2.9, has an optical spectrum comprising large number of modes with a fixed frequency gap between them. A mode-locked laser can produce OFCs directly, or they can be produced by modulating a single-frequency continuous wave (CW) laser. Some OFCs can cover more than an octave and span extremely broad bandwidths. When measured using an atomic reference, the fractional instability of the frequency of each OFC mode has been reported to be as

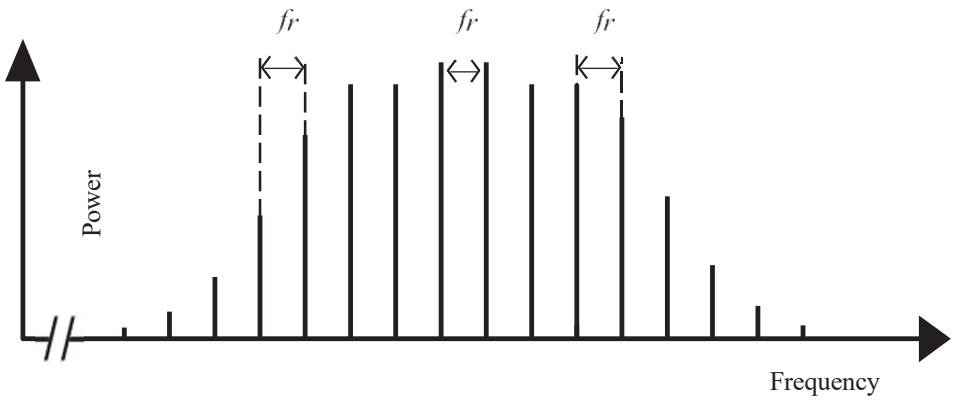

Figure 2.9. Spectrum of an Optical Frequency Comb. The comb modes are all separated by a repetition rate frequency, f_r.

low as 1.4 x 10^{-19} [69]. Because of its extremely high stability, the comb can be used as a "frequency ruler," measuring any frequency with high accuracy as long as it falls within the comb spectrum's bandwidth [70].

The OFC's capacity to convert optical to microwave frequencies is another essential component, making it a ground-breaking instrument for frequency metrology. Current sensors

cannot directly measure the frequency of the oscillating electrical field of an optical signal because they are far too slow. Instead, the unknown frequency is compared to a known frequency from an atomic transition to determine the frequency. A photodetector with adequate bandwidth may then measure the beat signal produced by the two signals, which is a down-conversion of their difference frequency.

As mentioned before, an OFC is typically generated by a mode-locked laser, which emits a train of ultra-short pulses. In the frequency domain, this pulse train corresponds to a comb of discrete frequencies :

$$f_n = f_{ceo} + n \cdot f_{rep} \tag{4}$$

where,

f_n represents the frequency of the n^{th} comb line, while f_{rep} denotes the repetition rate of the pulse train (spacing between comb lines), and f_{ceo} is the carrier-envelope offset frequency, which accounts for the phase shift between the pulse envelope and the carrier wave.

To use an OFC for precision measurements, both f_{rep} and f_{ceo} must be stabilized :

f_{rep} is locked using a photodetector and RF reference.

f_{ceo} is measured using an f-2f interferometer and locked to a reference.

Because the comb spacing can be fixed to a microwave reference, OFCs can directly connect the optical and microwave domains. As a result, the relative precision of each comb mode's frequency is equal to that of the microwave reference. This has significantly simplified optical frequency measurements and increased accessibility for non-metrology labs.

OFCs are also crucial spectroscopic tools because they may be used as a reference to precisely calibrate a higher power single frequency cw laser for use in conventional single laser spectroscopy [72]. Additionally, spectroscopic techniques utilize the full OFC spectrum, where various comb modes monitor multiple transitions concurrently [73],[74],[75]. Due to OFCs' ability, wavelengths that are useful for spectroscopy but difficult to reach with CW lasers, such as the ultraviolet and long wavelength infrared regimes, can be produced. Because of their incredible precision, regular spacing, and broad spectral coverage, OFCs can now be utilized in place of different gas discharge lamps to calibrate high-resolution astronomical spectrographs [76]. The simplicity with which OFCs can be amplified compared to gas lights is a less evident advantage for astronomical spectrometry. Bright sources like the Sun cannot have their spectrograms measured with long integration periods, which is necessary for low-intensity references [77]. Because of their exceptional stability, OFCs are also perfect for integrating optical atomic clocks. An optical counterpart, which operates at optical frequencies rather than microwave frequencies, uses an atomic (or molecule or ionic) transition as a reference, much like conventional microwave atomic

clocks. Compared to microwave clocks, optical atomic clocks can perform better since the frequency stability of a transition increases with frequency [78].

A fibre mode-locked laser OFC (FC1500-250-WG, Menlo Systems GmbH) with a central wavelength of 1560 nm and a repetition rate of 250 MHz was used for all of the experiments that employ the OFC as a master laser described in this thesis. The non-linear polarization rotation was the mode-locking process. The carrier envelope oscillator frequency and repetition rate were locked to a quartz oscillator (TimeTech GmbH).

This chapter provided an overview of the theoretical and technological foundations related to this research. We explored the principles of optical phase locking, noise characterisation, and the importance of OFCs. In addition, the chapter analyzed a number of phase-locking strategies, emphasizing the benefits and drawbacks of approaches including optical injection locking and optical phase-locked loops. Particular emphasis was placed on the challenges associated with locking tunable lasers, especially telecom-grade ITLA lasers to OFCs. Limited control bandwidth, increased intrinsic phase noise, and the requirement for low-cost, low-power solutions appropriate for scalable implementation are some of these difficulties. The necessity for a practical, reliable, and effective locking system that requires low optical power and doesn't require complex filtering or amplification was highlighted by the analysis of earlier research. This background sets the stage for the experimental investigations that follow. In the next chapter, we present a controlled benchmark experiment in which two identical tunable lasers are phase-locked to each other. This configuration allows us to evaluate the performance of the optical phase-locking system in isolation, before introducing the additional complexity of locking to an OFC. The results from this benchmark will serve as a reference for assessing the effectiveness of the OFC-locking approach developed later in the thesis.

Chapter 3

Locking Two Tunable Lasers

Building on the topic introduced in the previous chapter of optical phase locking, noise characterisation, and the importance of Optical Frequency Combs (OFCs), this chapter focuses on how these ideas are used in practice on the simple example of locking together two tunable lasers. The design of the two-laser phase-locking experiment was guided by the need to establish a controlled, simplified environment in which the core performance of the OPLL could be evaluated. It was crucial to confirm that the system could achieve and sustain phase coherence between two coherent optical sources before adding the complexity of locking a tunable laser to an OFC, which entails controlling numerous comb tones and ultra-low per- tone power levels. The experimental configuration for phase-locking two identical telecom- grade tunable lasers to one another is shown in this chapter. This configuration eliminates the complexity introduced by the comb's multiple tones and allows for a clear assessment of the phase-locking system's capabilities, including noise performance and stability. The results are used as a guide for assessing the performance of the OFC-locked system described in the subsequent chapter.

3.1 Objectives of Locking Two Tunable Lasers

. This configuration allowed us to :

- Evaluate the effectiveness of the Red Pitaya-based PLL [80] system.
- Investigate the minimum optical power required for stable locking.
- Understand the practical limitations of the tunable lasers, including their modulation bandwidth and phase noise characteristics.

This benchmark would later serve as a critical comparison point for assessing the performance of the OFC-locking system in Chapter 4. The methods and difficulties involved in attaining exact synchronization between two tunable laser sources will be examined in this chapter.

3.1.1 Emphasis on Practicality and Scalability

A key design philosophy of this work is to develop a phase-locking system that is not only high-performing but is also practical, compact, and cost-effective. The use of telecom-grade ITLA lasers, low-power operation, and a fully digital control loop implemented on a compact FPGA platform (Red Pitaya STEMLab 125-14) reflects this goal. The system was designed to:

- Use minimum optical power to function.
- Eliminate the requirement for high-speed electronics or complex analog circuits.
- Be easily reconfigurable and programmable for different locking scenarios.

This approach is in line with the broader vision of enabling scalable, comb-locked laser arrays for applications in coherent communications, photonic THz generation, and precision metrology [80].

3.1.2 Investigating Controller Architectures

Examining how controller architecture affects system performance was one of the key goals. There were two phases to the experiment:

- Single PI^2 Controller: This setup, which represented a traditional digital PLL with proportional and double-integrator feedback, acted as a baseline. It enabled us to evaluate the fundamental locking capability and pinpoint bandwidth and noise suppression constraints.
- Dual PI^2 Controllers (PI^4 Configuration): We desgned a higher-order controller by running two PI^2 controllers in parallel and combining their outputs. This configuration was created to address the drawbacks identified with the single PI^2 loop, namely with regards to enhancing long-term stability, reducing low-frequency phase noise, and increase the loop bandwidth.

From these two scenarios, conclusions can be made that there's trade-off among performance, complexity and stability in digital OPLL design.

3.1.3 Preparing for OFC Locking

Finally, this experiment was intended to prepare the system for the more demanding task of locking to an OFC. By understanding the behavior of the system in a simplified two-laser configuration, we could:

- Validate the signal detection and conditioning chain.
- Confirm the suitability of the Red Pitaya platform for real-time feedback control.

- Optimize the controller parameters for low-power operation.
- Identify and mitigate potential sources of instability or noise.

These insights directly informed the design and implementation of the OFC-locking experiment described in Chapter 4.

3.2 Experimental Setup

Figure 3.1 is the setup experiment that has been conducted. Tunable laser 2 (Slave laser) locks to Tunable laser 1 (Master laser). The objective of the experiment is to investigate the minimum power level of the Tunable laser 2 while it can still be locked to Tunable laser 1. By setting the output power of Tunable Laser 1 to 1 mW using a Variable Optical Attenuator (VOA), the output power of Tunable Laser 2 was then gradually reduced (20 nW, 10 nW, etc.) to determine the minimum level at which the two lasers could still maintain stable lock. Two parameters used to monitor the stability of the locked laser are the frequency error and phase noise.

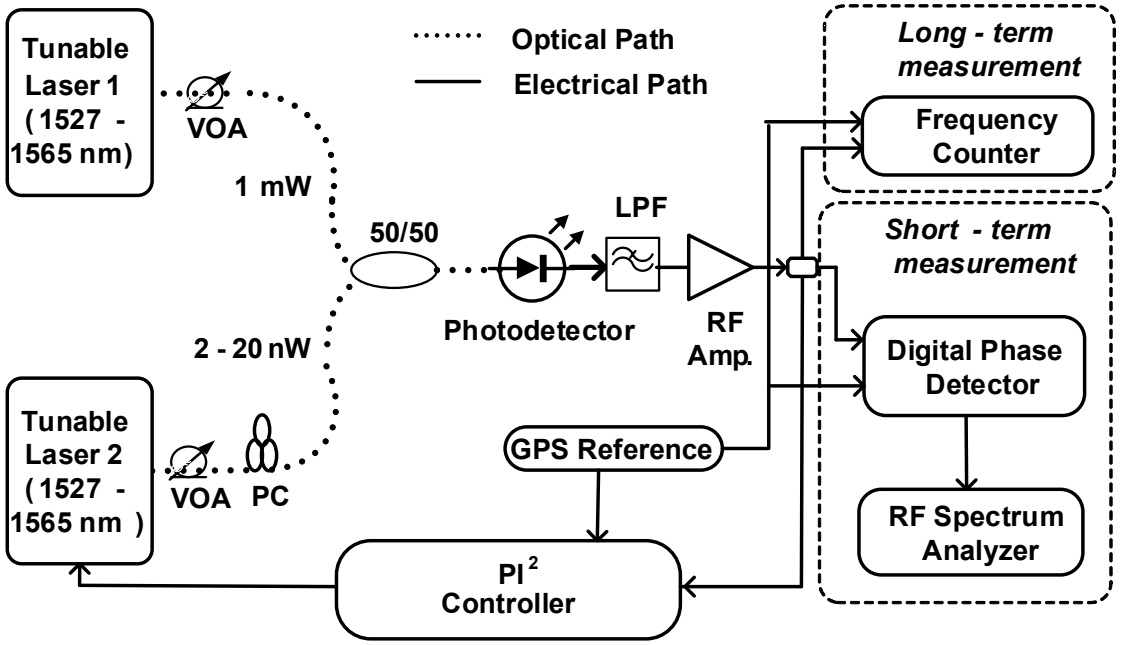

Figure. 3.1. Schematics of phase locking of two ITLA tunable lasers, one with power of 1 mW (0.5 mW reaching the photodetector after passing through the 50/50 coupler) and the other with low power, ranging from 0.5 nW (lowest power at which we achieved stable lock) to 10 nW (2-20 nW prior to the 50/50 coupler), using PI^2 feedback controller. VOA: Variable Optical Attenuator, PC: Polarization Controller, LPF: Low Pass Filter.

The loop filter, which is part of the OPLL as shown in figure 3.1, received the signal from the output of photodetector, which is an electrical signal. The Red Pitaya STEMLab 125-14 [81], as shown in figure 3.2, was used as the feedback controller. It is an embedded FPGA and microprocessor board, using a Python based software interface, providing complex acquisition and control schemes in an approximately 10 x 6 cm device, compact and inexpensive as well. Included are a ramp/scan signal generator, two Proportional – Integral^2 - Derivative (PI^{2}D) control filters, two lock-in amplifiers and an oscilloscope. The PID filters process the error signal and optimise the lock quality. PID filtering is the most common control system. PID control parameters can be set by adjusting the settings at the interface of the Red Pitaya. Optimisation of this parameters will minimise the error signal and then stabilize the system. Besides being a feedback controller, the OPLL of the two lasers was also implemented by the Red Pitaya STEMLab 125-14, with input frequency range of 60 MHz. Within the Red Pitaya, the analog voltage signals are converted to digital using two Analog to Digital Converters (ADC) , after processing, two Digital to Analog Converters (DCA) transform the digital signal to an output voltage on the range of 0 - 2 V. The resolution of the ADC/DAC is 14 bits, with a sampling rate of 125 MSa/s. So it is an all digital OPLL.

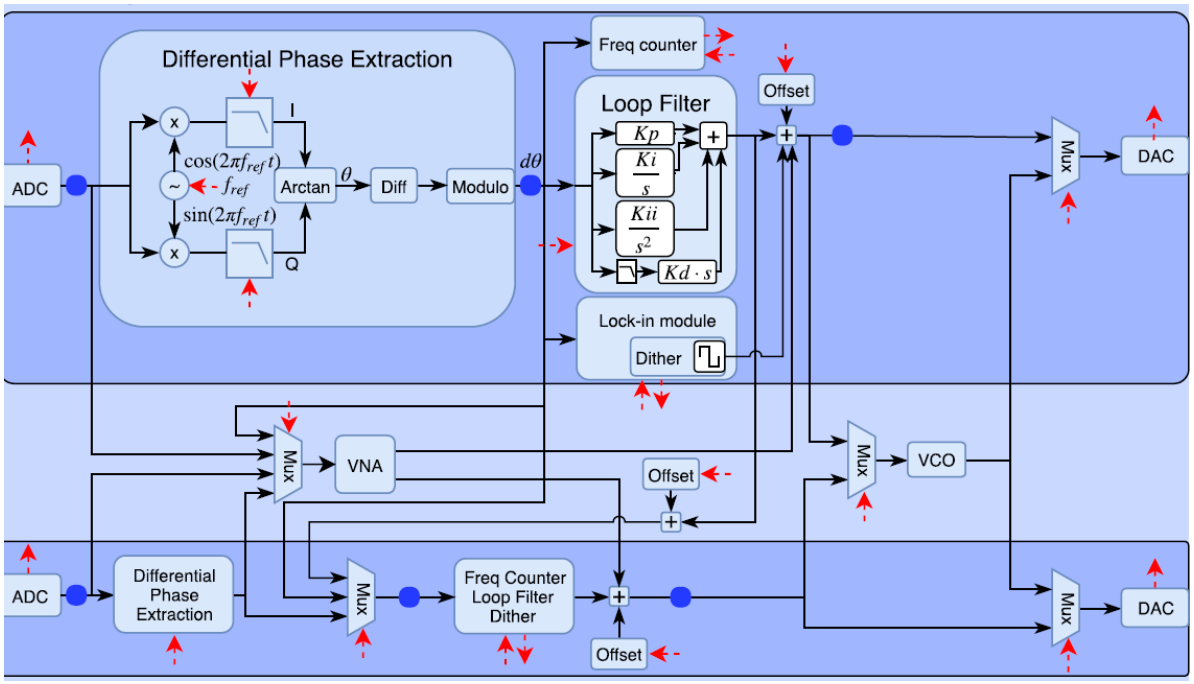

Figure 3.2. Block diagram of Red Pitaya STEMLab 125-14. Red arrows represent the communication with the PC software and blue dots represent the test points at which signals can be shown in the PC software. The second channel is a duplicate of the first. ADC: Analog-to-digital converter, MUX: Multiplexer, VNA: Vector network analyzer, VCO: Voltage-controlled oscillator, and DAC: Digital-to-analog converter.. The image was obtained from [10].

In the original Red Pitaya DPLL architecture presented by [10], the “Digital Loop Filter” block (Figure. 3.2) implements a general-purpose P/I/I/D controller (“PI²D”). This is the location in the firmware where the phase-error signal is processed following digital demodulation and numerical differentiation. In our system, the PI² controller corresponds directly to the proportional, integral, and double-integrator components already present within this block. Without changing the general DPLL signal-flow architecture, the PI⁴ controller created in this thesis is implemented by cascading two PI² filters internally within the same block, increasing the possible control bandwidth and low-frequency loop gain. Therefore, both PI² and PI⁴ configurations are situated entirely within the Digital Loop Filter module.

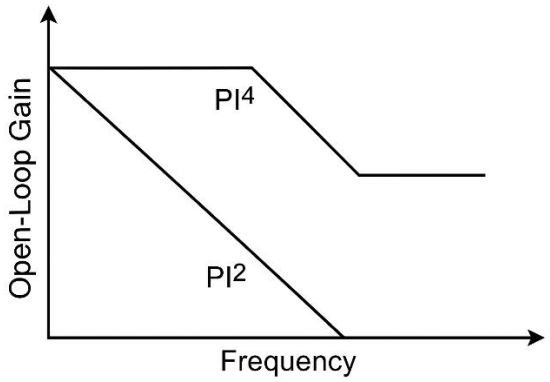

Figure 3.3. Open-loop gain spectrum.

A loop bandwidth of about 20 kHz results from the PI² controller's single dominating integrator region; beyond that, the gain drops below unity and the loop is unable to suppress phase variations. By cascading two PI² loops to create the PI⁴ controller, the low-frequency gain is increased by an additional 20–40 dB (shown graphically by the raised plateau), greatly increasing the effective unity-gain crossover to about 100 kHz. Long-term frequency stability and phase-noise suppression are directly improved by this increased loop bandwidth.

Cascading two PI² loops (PI⁴) introduces two independent low-frequency gain stages, resulting in a significantly stronger suppression of slow phase fluctuations compared to a single PI² loop. And as far as authors’ knowledge, no published work implements a PI⁴ (double-PI² cascade) inside the Red Pitaya PLL, nor in optical frequency-comb locking using telecom-grade tunable lasers.

Both Laser 1 and Laser 2 were Pure Photonics PPCL300 low-noise tunable lasers, supplied in an ITLA (Integrated Tunable Laser Assembly) package. These telecom-grade lasers are tunable across the C-band and provide an output power of up to 40 mW. The integrated nature of the laser provides a compact design. The laser can be tuned to any carrier frequency between 191.5 THz (wavelength of 1.565 µm) and 196.25 THz (wavelength of 1.528 µm). Output power of the lasers can be set between 6 - 16 dBm, controlled via an in-built semiconductor optical amplifier (SOA). A

low-pass filter (LPF) was used to filter the beat signal, and the filtered signal was then amplified by a low-noise RF amplifier. The Red Pitaya evaluation board's FPGA-based PI^2D (proportional, double-integral, derivative) controller received the amplified signal after that. [82]. A list of component parameter is given in Table 3.1

Table 3.1: Component parameters for Figure 3.1

Component	Parameter	Value
Laser 1 & Laser 2 PPCL300 Pure Photonics	Type	Continous mode
	Output power	+13 dBm
	Wavelength range (C-Band)	1527.6 – 1565.5 nm
	Operating temperature	0 - 70°C
	Connector type	FC/APC
	Fibre type	SMF-28
50/50 Coupler	Excess Loss	0.5 dB
	Connector type	FC/APC
	Fibre type	SMF-28
Photodetector	Model	MenloSystems FPD310
	Bandwidth	1 GHz
	Responsivity	0.9 A/W
	Gain Setting	5×10^4 V/W
	Operating temperature	10 - 40°C
	Optical input type	FC
Low pass filter (SLP-5+)	Cut-off frequency	50 MHz
Low Noise Amplifier (ZFL-500HLN)	Bandwidth	0.1 - 500 MHz
	Gain	24 dB (0.1 MHz)
	Noise Figure	2.9 dB (53.3 MHz)
10 MHz GPS Reference	Phase noise	–100 dBc/Hz at 1 Hz –150 dBc/Hz at 10kHz

Measurements were performed for various slave laser power levels ranging from 1 nW to 10 nW measurement at the photodetector input.

A high-precision frequency counter was used to assess the phase-locked tunable lasers' long-term frequency stability. This device is essential for measuring frequency error and drift over

long observation times. The frequency counter, Keysight 53230A, a universal counter with sub-millihertz averaging times in frequency measurement, was employed in this investigation. It was set up to track the nominally established beat frequency of 30 MHz between the two lasers. The frequency counter was referenced to a high-stabile RF source, ensuring that the measurement reflected the true stability of the laser system. The beat signal, after amplification and filtering, was fed directly into the frequency counter. A gate time of 1 second was used for most measurements, providing a balance between resolution and temporal granularity. For Allan deviation analysis purposes, shorter gate times (e.g., 4 µs) were also employed to capture frequency fluctuations across a wide range of averaging intervals. The frequency counter provided the following key metrics:

- **Instantaneous frequency error**: The deviation of the measured beat frequency from the nominal 30 MHz value, recorded over time.
- **Peak-to-peak frequency variation**: Used to assess the stability of the phase-lock over long durations (e.g., 10 hours).
- **Allan deviation**: This method helps track how frequency stability shifts as the averaging time changes. This approach makes it easier to identify what kind of noise is present in the system, whether it's flicker, random walk, or white phase noise.

3.3 Lock Acquisition and Stability Behavior

To confirm the OPLL system is functioning properly, it's important to keep the two tunable lasers consistently phase-locked.

3.3.1 Lock Acquisition Process

We began the locking process by carefully adjusting the lasers so that their beat frequency settled near 30 MHz, which is the target intermediate frequency. After that, we followed a series of steps to get the system locked in :

- Initial Wavelength Tuning:

We used the lasers' built-in controls to manually bring their wavelengths reasonably close, just a few gigahertz apart. Fine tuning was performed to bring the beat frequency close to the 30 MHz offset target.

- Polarization Matching:

To improve how well the visibility of the beat signal at photodetector, a polarization controller was used to align the polarization of the master and slave laser outputs. In order to provide a robust and consistent interference signal, this step was important.

- Controller Activation:

After switching on the digital PI^2 or PI^4 controller, it started working on the error signal and sent feedback to adjust the phase modulation input of the slave laser.

3.3.2 Indicators of Successful Locking

Several indicators were used to verify that the system had achieved and maintained phase- lock:

- Spectral Signature:

The RF spectrum analyser showed a narrow linewidth peak at 30 MHz, i.e. 200 kHz, which suggested that the two lasers were beating. The absence of sidebands or frequency drift confirmed the stability of the lock.

- Phase Detector Output:

The digital phase detector demonstrated that the controller was successfully minimising the phase error by producing a clear, low-noise signal.

- Frequency Counter Readings:

While monitoring the system, we noticed that the frequency counter consistently showed a fairly beat frequency. The signal was perfectly flat, of course there were small fluctuations from peak to peak but nothing unexpected.

- Visual Oscilloscope Trace:

On the oscilloscope, the beat signal appeared as a stable sinusoidal waveform, exhibiting no noticeable jitter or amplitude modulation. On the oscilloscope, the beat signal appeared as a steady sinusoidal waveform, no jitter or amplitude modulation.

3.3.3 Lock Robustness and Stability

After being obtained, the lock was largely reliable and could be kept up without intervention for a number of hours. The mechanism showed resistance to small environmental disruptions such as:

- Small temperature fluctuations in the lab environment.
- Mechanical vibrations from nearby equipment.
- Minor power fluctuations in the laser or control electronics.

However, the lock could be disrupted by:

- Sudden changes in laser drive current or temperature.
- Significant misalignment of polarization.
- Excessive attenuation of the slave laser signal below 1 nW.

Significantly improved lock robustness was offered by the PI^4 controller architecture, especially at low power levels and in the presence of environmental noise. It also allowed for faster recovery in the event of temporary lock loss.

3.4 Challenges and Mitigation Strategies

The phase-locking setup for the two tunable lasers was deliberately constructed to be simple and easy to control. However, once constructed and tested, several practical issues became apparent. .These were just minor inconveniences, they stemmed from the behaviour of the laser in real time, level of sensitivity of the system to its surroundings, etc. The following subchapter discusses these main issues and the ways to minimize or solve them.

3.4.1 Challenge 1: Low Signal-to-Noise Ratio at Minimal Power Levels

Problem:

One of the primary goals of the experiment was to determine the minimum optical power at which stable locking could be achieved. As the slave laser power was reduced to the nanowatt level (1–10 nW), the beat signal at the photodetector became increasingly weak, leading to a low signal-to-noise ratio (SNR). This made it difficult for the controller to extract a clean error signal, especially in the presence of environmental noise.

Mitigation:

- A high-gain, low-noise RF amplifier (Mini-Circuits ZFL-500HLN+) was used immediately after the photodetector to boost the beat signal before digitization.
- The photodetector was properly biased and operated within its optimal input power range to avoid saturation or under-response.

3.4.2 Challenge 2: Limited Modulation Bandwidth of Tunable Lasers

Problem:

The system loop bandwidth cannot exceed 100 kHz because it is limited by the modulation bandwidth of the ITLA C-band telecom-grade lasers (approximately 100 kHz).

Mitigation:

- The controller parameters were carefully tuned and optimized to match the laser's modulation response, avoiding instability due to bandwidth mismatch.
- The PI^4 controller was configured to add loop gain and supress the low frequency phase noise

3.4.3 Challenge 3: Lock Acquisition Sensitivity

Problem:

The system setup capability to lock the two lasers was depend on initial state, including the offset frequency between the two lasers and the controller's initial parameters. If the frequency of the two lasers is too far apart, the controller can not converge the locked state.

Mitigation:

- A methodical lock acquisition process that included incremental power adjustment, polarization alignment, and coarse wavelength tuning was developed.
- The Red Pitaya PLL was used to monitor the error signal and modify the controller gains in real time during lock acquisition.
- A 30 MHz synthesizer was used as a reference to ensure consistent beat frequency targeting.

These mitigation strategies were essential for reliable and consistent locking performance. The design of the more intricate OFC-locking system, which is covered in the following chapter, was influenced by the knowledge obtained by tackling these difficulties. The presence of many comb tones and even lower per-tone power levels accumulated similar problems.

Besides the three challenges above, there is also polarization misalignment. The beat signal strength is highly sensitive to the polarization alignment of the two laser beams. The interference contrast is decreased by any mismatch in polarization states, which weakens the beat signal and may possibly make lock acquisition impossible. In order to overcome these difficulties, a manual polarization controller (PC) was added to the slave laser's optical path so that its polarization matched that of the master laser. By enhancing the beat-signal amplitude on the RF spectrum analyzer, the alignment was adjusted. Once optimal alignment was achieved, the fiber paths were secured to minimize polarization drift arising from mechanical disturbances or thermal fluctuations.

The performance of a digital optical phase-lock loop (OPLL) depends significantly on how its feedback controller is designed and tuned. In our experiment, we explored two different configurations to understand their impact on system behavior. One setup used a single PI^2 controller, which combines proportional control with a double integrator, while the other stacked two of these controllers to form a PI^4 configuration. This was just a theoretical comparison, we looked at how each setup behaved in practice, focusing on how quickly and reliably they acquired lock, how they responded to disturbances, and how usable they were in a real lab setting. The results revealed clear differences in responsiveness and stability, which are discussed in detail in the following sections.

3.4.4 Lock Acquisition Behavior

PI^2 Controller:

Lock acquisition using a single PI^2 controller was generally reliable when the initial frequency offset between the lasers was small and the signal-to-noise ratio was high. However, the system was more sensitive to initial conditions, and achieving lock at very low power levels (e.g., 1–2 nW) required careful tuning and environmental stability.

PI^4 Controller:

Faster and more reliable lock acquisition was shown by the PI^4 configuration. Even in less ideal circumstances, successful locking was made possible by the system's increased ability to aggressively rectify phase mistakes due to the increased loop gain and bandwidth. Lock acquisition was more tolerant to initial frequency offsets and environmental disturbances.

3.4.5 Stability and Robustness

PI^2 Controller:

Under controlled circumstances, the system remained stable after locking. However, because of ambient noise or gradual phase drifts that went beyond the controller's compensation range, it was more prone to drift and sporadic lock loss.

PI^4 Controller:

The PI^4 controller significantly improved lock robustness. It was more resistant to low- frequency noise and slow drifts, and it was able to retain phase-lock for longer periods of time. This was especially noticeable when the frequency inaccuracy was firmly constrained during long-term monitoring.

3.4.6 Noise Suppression

PI² Controller:

It managed to reduce phase noise to a moderate extent, It performed reasonably well around the mid-range offsets. But at the lower end of the frequency spectrum, the performance started to fall apart. We figured that was likely due to the limited bandwidth only about 20 kHz, which just wasn't enough to handle those frequencies effectively.

PI⁴ Controller:

Delivered superior noise suppression across a broader frequency range. The extended bandwidth (~100 kHz) allowed for better attenuation of both low- and mid-frequency phase noise components. This resulted in a visibly cleaner beat signal and lower integrated phase jitter.

3.4.7 Ease of Tuning

PI² Controller:

Relatively easy to tune because the configuration is simple, and that will impact to relatively fast setup.

PI⁴ Controller:

More careful tuning was necessary since the two PI² loops' interactions had to be matched. But after it was adjusted, it performed noticeably better and, with a few small adjustment, could be used in various locking situations.

3.4.8 Practical Implications

The PI² controller is appropiate for basic locking tasks where simplicity and ease of implementation are priorities.

As for the PI⁴ controller is better suited for applications requiring high stability, low noise, and robust performance under varying conditions.

This qualitative comparison highlights the importance of controller architecture in digital OPLL systems. For sophisticated applications like OFC-locking, which is covered in the following chapter, the PI⁴ configuration is the recommended option due to its significant performance gains, even though the PI² controller offers a working baseline.

3.5 Implications for OFC Locking

The successful implementation and evaluation of phase-locking between two tunable lasers provides critical insights and practical groundwork for the more complex task of locking a tunable laser to an optical frequency comb (OFC), which is the focus of the next chapter. While the two-laser configuration serves as a simplified model, it shares many of the core challenges and dynamics present in OFC-based locking. This section outlines the key implications of the two-laser experiment for OFC locking in terms of system design, control strategy, and performance expectations.

3.5.1 Validation of the Digital Control Architecture

Through the two-laser setup, we confirmed that a fully digital OPLL built on a compact FPGA board (Red Pitaya STEMLab 125-14) can reliably achieve stable and accurate phase locking. This validation is crucial for OFC locking, where the same digital architecture must handle more complex beat signals and operate at even lower signal levels.

- We found that Red Pitaya handled phase error signals in real time. It didn't just digitize and process the data, it also responded quickly and reliably during testing. This real-time performance was especially noticeable when the system was under typical operating conditions, showing that the device could keep up without lag or instability.
- Because of the flexibility of the FPGA platform, switching between PI^2 and PI^4 controllers was quick and straightforward, a key advantage when adapting to varying OFC conditions.

3.5.2 Importance of Controller Design

Looking at both the PI^2 and PI^4 controllers made it clear how crucial loop gain and bandwidth are for maintaining solid, reliable locking, especially when dealing with limited modulation bandwidth and high phase noise, conditions that are even more pronounced in OFC locking.

- The PI^4 controller's superior performance in suppressing low-frequency noise and maintaining lock at low power levels directly informs the controller choice for OFC locking.
- The tuning strategies developed here will serve as a starting point for optimizing the controller in the OFC context.

3.5.3 Power Sensitivity and Signal Conditioning

The experiment demonstrated that stable locking could be achieved with slave laser powers as low as 1 nW. This is particularly relevant for OFC locking, where the power per comb tone is inherently low due to the broad spectral distribution of the comb.

- The signal conditioning chain, comprising the photodetector, low-pass filter, and RF amplifier, was validated for low-SNR operation.
- These components will be reused in the OFC setup, with confidence that they can handle the weak beat signals typical of comb-based locking.

3.5.4 Environmental and Practical Considerations

The challenges encountered and mitigated in the two-laser setup—such as polarization alignment, environmental noise, and lock acquisition sensitivity—are all expected to be present in the OFC locking scenario, often in more severe forms.

- The procedures developed for polarization control, power balancing, and lock acquisition will be directly applicable.
- The robustness of the PI^4 configuration to environmental disturbances shows it will be well-suited for the more demanding OFC environment.

3.5.5 Benchmark for Performance Comparison

Lastly, the results of the two-lasers locking each other provided quantitative and qualitative standard by which the OFC-locked system's performance may be evaluated. Parameters like:

- Minimum locking power,
- Phase noise suppression,
- Integrated jitter,
- Frequency stability (e.g., Allan deviation),

will be compared between the two configurations to assess the impact of comb-based locking and to validate the scalability of the system.

In summary, The two-laser phase-locking experiment established the methodological and technical groundwork for the more intricate OFC-locking experiments in addition to proving that low-cost, digital control systems may be used for high-precision optical locking. The design, implementation, and optimization of the OFC-locked system described in Chapter 4 will be guided by the knowledge acquired here.

To evaluate the performance of the phase-locking system under controlled conditions, we conducted a series of experiments using two identical telecom-grade tunable lasers. These lasers were phase-locked to each other to establish a benchmark for system performance before introducing the complexity of locking to an optical frequency comb (OFC). Like mentioned earlier in the beginning of the chapter, we conducted two different experiments setup, first setup : Locking with a Single PI^2 Controller as shown in figure 3.1. In the first configuration, the feedback loop was implemented using a single proportional–double- integrator (PI^2) controller. This controller was programmed on a Red Pitaya FPGA platform and used to process the beat signal generated by the interference of the two lasers.

- **Beat Frequency** : The lasers were offset by 30 MHz to generate a stable beat signal.
- **Signal Conditioning** : The beat signal was filtered and amplified before being digitized by the FPGA.
- **Feedback Path** : The PI² controller generated a correction signal that was applied to the phase modulation input of the slave laser.

The purpose is this arrangement used as a baseline to examine the performance of a standard digital phase-lock loop (PLL) in suppressing phase noise and maintaining frequency stability, with the limitations that the control bandwidth was limited by the loop gain and the inherent delay in the digital processing chain.

To overcome the limitations observed with a single PI² controller, two PI² controllers working in parallel were used in a second experiment as shown in figure 3.4 or figure 3.5 (laboratory experiment). By combining the output of each PI² loop, a PI⁴ controller was essentially built, increasing the loop's overall gain and bandwidth.

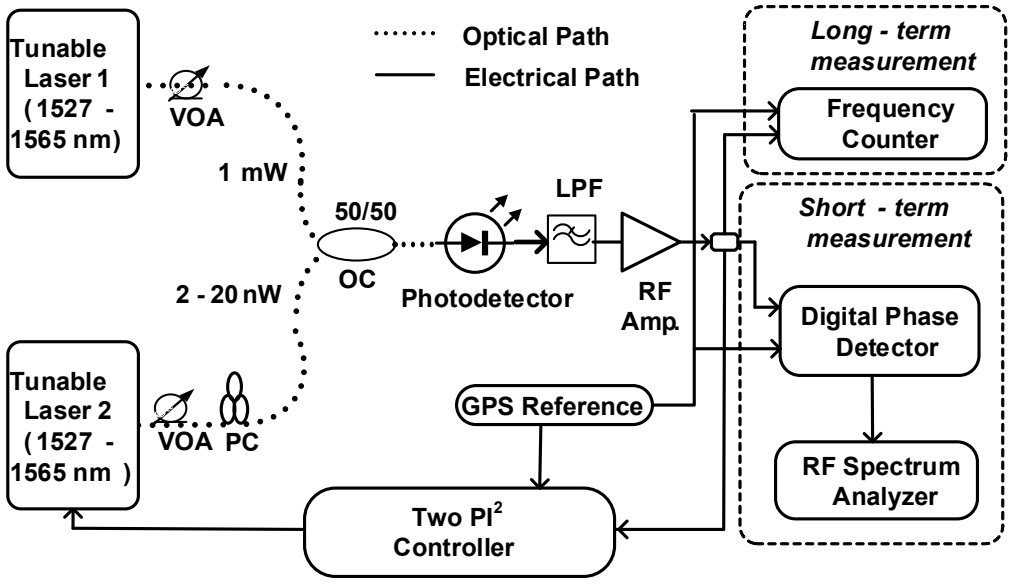

Figure. 3.4. Schematics of phase locking of two ITLA tunable lasers, one with power of 1 mW and the other with low power, ranging from 1 nW (lowest power at which we achieved stable lock) to 10 nW (2-20 nW prior to the 50/50 coupler), using **two PI² controller**. VOA: Variable Optical Attenuator, PC: Polarization Controller, LPF: Low Pass Filter.

- The Red Pitaya board, which supports two independent input/output channels, was configured to run two identical PI^2 controllers. The beat signal was divided and routed to both controllers, with their outputs later combined using a passive RF combiner. By using the PI^4 configuration, we were able to boost the loop gain at lower frequencies while keeping the system stable, which helped suppress phase noise more effectively. It compensates for the limited control authority of telecom-grade tunable lasers, which typically have lower modulation efficiency and narrower control bandwidths than laboratory-grade lasers. The corresponding noise-characterisation results, including phase-noise suppression, integrated jitter, and frequency-stability analysis (e.g., Allan deviation), are presented and discussed in Chapter 5.

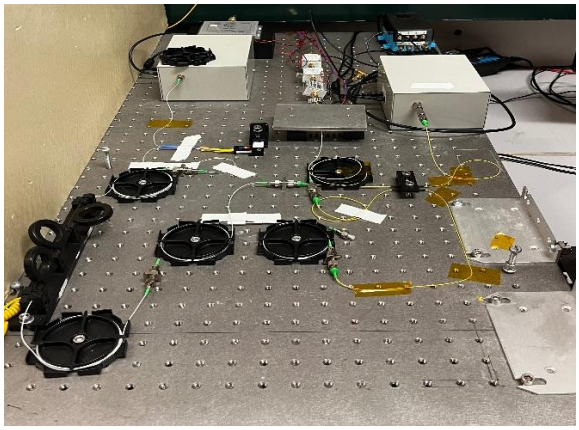

Figure 3.5. Laboratory experiment for phase locking of two ITLA tunable lasers.

3.6 Laser Modulation Bandwidth

To measure our tunable laser modulation bandwidth, we use the setup in Figure 3.6 shown below,

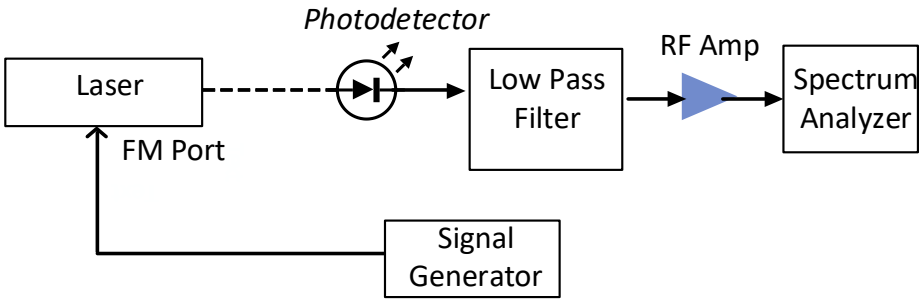

Figure. 3.6. Schematics for laser modulation bandwidth measurement.

We use RF signal generator to apply a small sinusoidal modulation current to the laser. The output of the laser is then sent to photodetector. After being sent through LPF and RF Amplifier, the signal is analyzed using a RF Spectrum analyzer. We measured the modulation transfer function by evaluating the output power as a function of modulation frequency. The 3 dB bandwidth corresponds to the frequency at which the response decreases by 3 dB relative to its low-frequency level.

The results plotted in Figure 3.7, shows that the laser modulation bandwith is 100 kHz, where the 3 dB drop occurred.

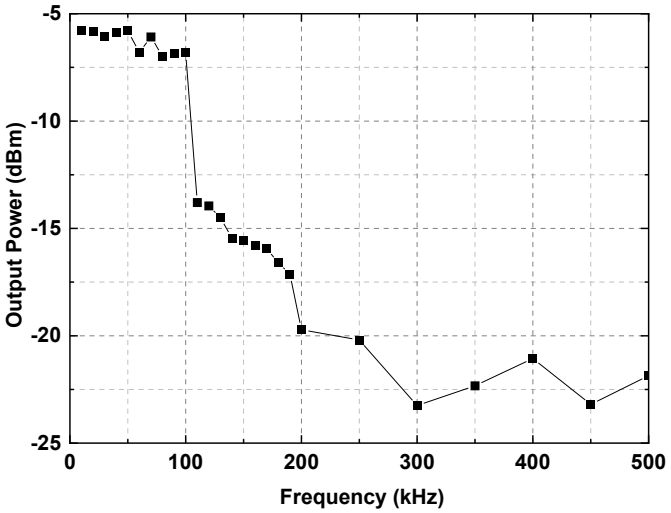

Figure. 3.7. Laser modulation bandwidth.

From the experiment setup shown in Figure 3.1, where we use 1 PI^2 Controller, we characterize the phase noise for different output powers of Laser 2 and across different wavelengths. (Figure 3.8 shows the minimum output power of Laser 2 where the two lasers can still lock is 1 nW (-60 dBm).

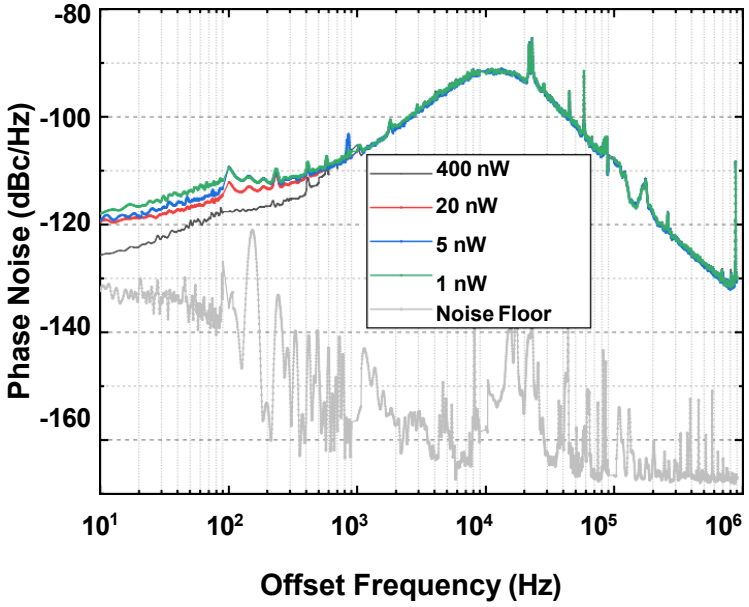

Figure. 3.8. Phase Noise of beat signal of locking 2 Lasers together with different output power of Laser 2 (Slave Laser).

Figure 3.8 presents the phase-noise performance of two phase-locked tunable lasers across three wavelengths (1530 nm, 1550 nm, and 1565 nm). The results indicate that the phase-noise behaviour is consistent across all measured wavelengths. We can conclude that the phase-noise characteristics show negligible differences given by C-Band.

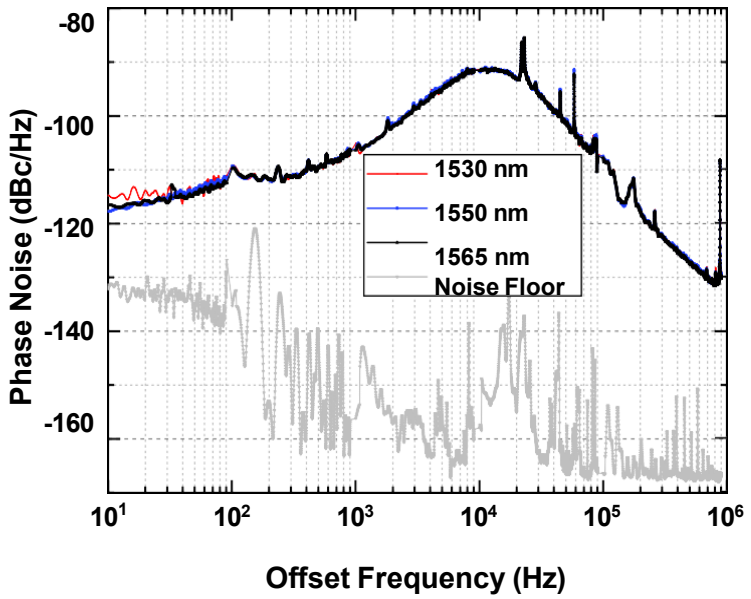

Fig. 3.9. Phase Noise of beat signal of locking two tunable lasers across different wavelength.

From both graphs, Figure 3.8 and Figure 3.9, we can see that the loop bandwidth is 20 kHz as opposed to the 100 kHz modulation bandwidth of the laser. Employing two PI^2 Controller as show in experiment of setup in Figure 3.3. Figure 3.8 shows the phase-noise spectrum measured when the two tunable lasers are phase-locked to each other.

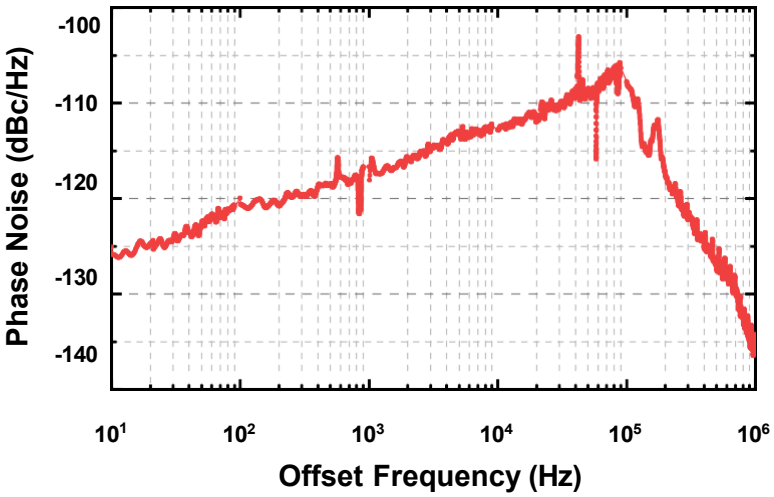

Figure. 3.10. Phase Noise of beat signal of locking two tunable lasers using 2 PI^2 Controller.

The result shows that by using 2 PI^2 Controller, the loop bandwidth of the system is enhanced, from 20 kHz 100 kHz, as we expected.

This chapter presented the design, implementation, and qualitative evaluation of a digital optical phase-lock loop (OPLL) system for locking two telecom-grade tunable lasers. As a fundamental benchmark, the experiment enabled us to verify the digital control architecture's performance, evaluate the influence of controller design, and investigate the real-world difficulties in attaining stable phase-locking at low power levels.

Important lessons learned from this chapter include:

- We used the Red Pitaya STEMLab 125-14 to build a fully digital OPLL, which successfully kept the two tunable lasers phase-locked throughout the test.
- In this setup, the system was able to stay locked even when the slave laser power was reduced to just 1 nW, which shows it can handle low signal conditions.
- The PI^4 controller proved to be more effective than the simpler PI^2 version, it locked faster, handled noise better, and stayed stable over longer periods.
- Practical challenges such as polarization alignment, environmental noise, and limited modulation bandwidth were identified and effectively mitigated through careful system design and tuning.

The experiment provided a controlled environment to develop and refine procedures for lock acquisition, controller tuning, and system stabilization, procedures that are directly applicable to more complex locking scenarios. Most importantly, this chapter established a performance baseline and a set of validated techniques that will be carried forward into the next phase of this research: locking a tunable laser to an optical frequency comb (OFC). While the two-laser configuration involved a single, clean beat signal, OFC locking introduces new complexities, including the presence of multiple comb tones, ultra-low per-tone power levels, and the need for broader spectral compatibility.

In the next chapter, we take the OPLL system a step further by applying it to a more challenging case. We'll look at how the earlier strategies, especially the PI^4 controller and low- power signal conditioning, help achieve stable and scalable locking to an OFC. This transition marks a critical step toward realizing practical, comb-locked laser systems for advanced photonic applications.

Chapter 4

Locking A Tunable Laser to an Optical Frequency Comb

In the previous chapter, we demonstrated optical phase-locking loop of two telecom- grade tunable lasers that are identical. By using this setup as a controlled benchmark, we were able to assess the phase-locking system's performance in terms of long-term frequency stability, jitter, and phase noise. The results showed that stable locking could be achieved with minimal optical power and that the use of a PI^4 controller significantly enhanced system performance. These results prepared the way for applying the locking technique to more complex and practical situations. This chapter moves forward by focusing on the primary objective of this research: the phase-locking of a tunable laser to an optical frequency comb (OFC). Unlike the two-laser configuration, locking to an OFC presents additional challenges because it involves multiple comb tones, each separated by a fixed frequency interval. The beat signal generated in this case results from the interference between the tunable laser and all nearby comb lines, which can complicate signal detection and feedback control.

Apart from the challenges, there are some benefits to locking a tunable laser to an OFC [85]. It makes it possible to create a single-frequency optical signal that is extremely stable and inherits the comb's frequency precision and stability. Additionally, continuous wavelength control across the laser's tuning range can be achieved by adjusting the offset frequency between the laser and the comb tone. This is a crucial feature for applications in photonic THz generation [86] and coherent communications .

This chapter presents the design, implementation, and characterization of a system for locking a telecom-grade tunable laser to an OFC using the same low-cost digital electronics platform introduced earlier. We describe an experimental setup that uses a broadband photodetector to collect the beat signal without the need of tunable optical filters. We then evaluate the system's performance by examining phase noise, frequency stability, and robustness at various wavelengths and comb tone levels.

4.1 Objectives

The complexity, accuracy, and practical significance of locking a tunable laser to an optical frequency comb (OFC) has advanced significantly from locking two tunable lasers. The requirement to show that a low-cost, digitally controlled phase-locking system might be expanded to function dependably in the more demanding setting of OFC-based locking served as the impetus for the design of this experiment. The main driving forces, design tenets, and experimental objectives that influenced the creation of the OFC-locking system are described in this section.

4.1.1 Key Design Principles

The system was designed around the following core principles:

- Low-Power Operation: The system targets stable locking with per-tone OFC powers as low as 1 nW. This is critical for practical deployment, where OFC power must be shared among many channels.
- Digital Control: The use of a Red Pitaya FPGA platform [89] allows for flexible, control using a PI^4 feedback architecture. This digital approach ensures precise, real-time phase correction and simplifies integration with other systems.
- Robustness and Tunability: The system must stay steady in the face of environmental variations and keep lock throughout the laser's entire C-band tuning range. Continuous wavelength control requires the capacity to adjust the offset frequency between the laser and the comb tone.

4.1.3 Experimental Objectives

The specific objectives of this experiment were:

- To demonstrate stable phase-locking of a telecom-grade tunable laser to an OFC using a fully digital feedback loop and minimal optical power.
- To validate the use of the entire OFC spectrum without pre-filtering, thereby simplifying the optical setup and reducing cost.
- To evaluate the performance of the PI^4 controller in the presence of multiple comb tones and low SNR conditions.
- To assess the system’s robustness across different wavelengths and comb tone powers, confirming its suitability for scalable, multi-laser locking.
- To prepare for quantitative noise characterization, which will be addressed in Chapter

5, by ensuring that the system can maintain lock over long durations and under varying conditions.

This design philosophy reflects a shift from proof-of-concept to practical implementation. This work establishes the basis for accessible and versatile scalable high-performance photonic systems by showing that a single OFC may function as a stable reference for multiple tunable lasers.

4.2 Experimental Methodology

The experimental setup for phase-locking a telecom-grade tunable laser to an optical frequency comb (OFC) is thoroughly described in this section. The four main subsystems of the technique are measurement, control, detection, and optical. Each subsystem is described in detail to ensure reproducibility and to highlight the design considerations that enabled robust locking at ultra-low optical power levels.

4.2.1 Optical Subsystem

The optical subsystem is responsible for generating and combining the signals from the tunable laser and the OFC.

- Optical Frequency Comb (OFC):
  - ✓ Source: Menlo FC1500 mode-locked fiber laser.
  - ✓ Output: Broad spectrum with 77 nm (10 dB width) centered in the C-band. (shown in figure 4.1 below)

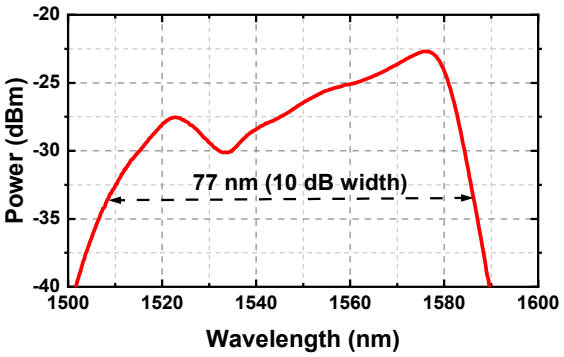

Figure. 4.1. Spectrum on the used OFC with total power of 0.5 mW and per-comb powers of 1.1 nW at 1530 nm, 2.3 nW at 1550 nm, and 3.7 nW at 1565 nm.

Instead of using the whole 10 dB or –3 dB optical power envelope commonly employed in metrology, the spectral bandwidth of OFC used in this study is defined as the wavelength range across which the comb tones produce sufficient optical power to ensure reliable phase locking. Only a portion of the measured OFC spectrum, which spans about 77 nm (10 dB width) surrounding the C-band (Fig.

4.1), offers tone powers at or above the minimal locking threshold of 1 nW. The functional bandwidth of the comb is better described by the region in which the per-tone power exceeds this minimum usable level because the detected beat-note SNR is what essentially limits the locking performance, and the beat-note SNR is directly proportional to the optical power of the nearest comb mode.

For instance, the tone power fluctuates from 1.1 nW to 3.7 nW throughout the 1527–1565 nm range used in this thesis, which is adequate for reliable locking without optical amplification or filtering. Outside of this area, the optical spectrum still shows detectable amplitude, but the tone power falls below the locking threshold, which will cause the locking unstable or even unlock. For this reason, the OFC bandwidth relevant to this work is defined by per-tone power usability, not simply by spectral envelope width.

As for the loop bandwidth of an optical phase-locked loop, it is defined as the frequency at which the closed-loop transfer function of the PLL falls to –3 dB relative to its low-frequency (DC) gain. In other words, it is the highest frequency of phase fluctuations on the slave laser that the loop can effectively suppress. Beyond the loop bandwidth, the controller cannot respond quickly enough, and the slave laser behaves increasingly like a free-running device.

- ✓ Comb spacing: 250 MHz.
- ✓ Per-tone power: 1–3 nW.
- ✓ Output is delivered via SMF-28 fiber with FC/APC connectors.

- Tunable Laser:
  - ✓ Device: Commercial ITLA (Integrated Tunable Laser Assembly).
  - ✓ Wavelength range: 1527.6–1565.5 nm.
  - ✓ Output power: Up to 40 mW; ~1 mW tapped for locking.
  - ✓ Operated in continuous-wave mode.
- Combining and Conditioning:
  - ✓ A 50/50 optical coupler combines the OFC and tunable laser outputs.
  - ✓ A Variable Optical Attenuator (VOA) adjusts the OFC power to ~2 nW per tone.
  - ✓ A Polarization Controller (PC) ensures optimal polarization alignment for interference.

4.2.2 Detection Subsystem

This subsystem extracts the beat signal between the tunable laser and the nearest comb tone.

- Photodetection:
  - ✓ Device: Menlo FPD310 high-speed photodetector.
  - ✓ Bandwidth: 1 GHz.
  - ✓ Responsivity: 0.9 A/W.
  - ✓ Beat signal typically centered at 30 MHz.
- Filtering and Amplification:
  - ✓ A 50 MHz low-pass filter (LPF) removes high-frequency noise and unwanted beat components.
  - ✓ A low-noise RF amplifier (Mini-Circuits ZFL-500HLN+) boosts the filtered signal.
  - ✓ Amplified signal is split into three paths for control and measurement.

4.2.3 Control Subsystem

This subsystem implements the feedback loop that maintains phase lock of tunable laser and OFC.

- Digital Phase Detector:
  - ✓ Measures phase error between the beat signal and a 30 MHz reference.
- PI^4 Controller:
  - ✓ Two parallel PI^2 controllers form a PI^4 loop.
  - ✓ Enhances loop bandwidth and phase noise suppression.
  - ✓ Output modulates the phase section of the tunable laser.
- Reference Signal:
  - ✓ A 30 MHz synthesizer provides the reference tone.
  - ✓ Locked to a 10 MHz GPS-disciplined oscillator for long-term stability.

4.2.4 Measurement Subsystem

This subsystem monitors the performance of the locking system in both short and long time scales.

- Short-Term Analysis:
    - ✓ Beat signal is analyzed using Digital Phase Detector and RF spectrum analyzer.
    - ✓ Phase noise and spectral purity are evaluated.
- Long-Term Stability:
    - ✓ Frequency counter tracks the beat frequency over time.
    - ✓ Allan deviation and frequency drift are computed.

Figure 4.2 presents the schematic of the experimental setup used to phase-lock a telecom- grade tunable laser to an OFC. This configuration builds upon the two-lasers locking setup described in Chapter 3, with the key difference being the replacement of one tunable laser with a broadband OFC source.

As mentioned above, the OFC used in this setup is a Menlo FC1500 oscillator, emitting a broad spectrum with a 77 nm full-width at half-maximum (FWHM) and a comb line spacing of 250 MHz. The total output power is approximately 0.5 mW, with individual comb tones having powers as low as 1–3 nW. A commercial Integrable Tunable Laser Assembly (ITLA) operating in the C-band (1527–1565 nm) is used. The laser provides up to 40 mW of output power. A small portion of this power (approximately 1 mW) is tapped off for phase-locking purposes, while the majority remains available for downstream applications. The tapped signal from the tunable laser and the OFC output are combined using a 50/50 optical coupler. This generates a beat signal between the tunable laser and the nearest comb tone(s). The combined optical signal is detected using a high-speed, amplified photodetector (Menlo FPD310), which has a bandwidth of 1 GHz. The beat signal, typically centered at 30 MHz, is extracted from the photodetector output.

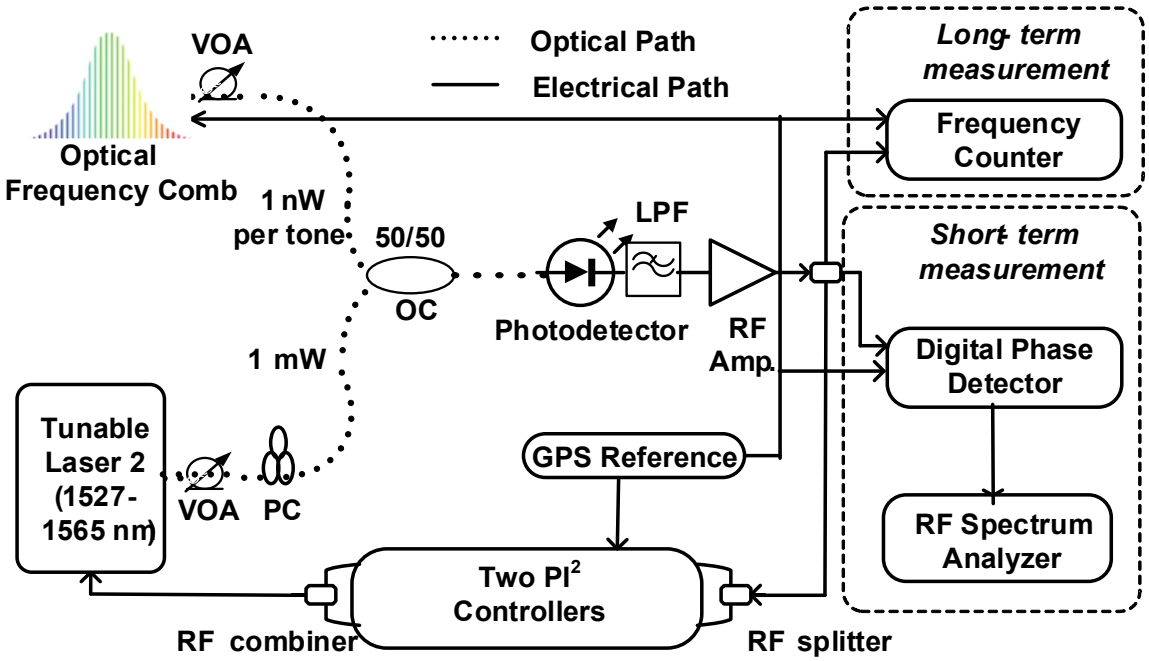

Figure. 4.2. Schematic of the phase locking of an ITLA tunable laser to an OFC with power set at 1 nW for comb tone used for locking (0.5 nW reaching the photodetector). VOA : Variable Optical Attenuator, PC : Polarization Controller, LPF: Low Pass Filter.

A 50 MHz low-pass filter is used to isolate the desired beat frequency and suppress high- frequency noise and unwanted beat components from other comb tones. The filtered beat signal is amplified using a low-noise RF amplifier (Mini-Circuits ZFL-500HLN+) to ensure sufficient signal strength for subsequent processing. The amplified signal is split into three paths, one path is sent to a digital phase detector for short-term phase noise analysis, another path is sent to a frequency counter for long-term frequency stability measurements, the third path is used as the feedback input to the phase-lock loop controller. The feedback loop is implemented using a Red Pitaya board with a Xilinx Zynq 7010 FPGA [90]. Two independent PI^2 (proportional–double-integrator) controllers are used in parallel to form a PI^4 controller. This configuration enhances loop bandwidth and improves phase noise suppression. The controller modulates the phase section of the tunable laser to maintain a fixed offset (30 MHz) from the selected comb tone. As for Variable Optical Attenuator (VOA) and Polarization Controller (PC), These components are used to fine-tune the optical power and polarization state of the OFC signal before it enters the coupler, ensuring optimal interference and beat signal quality.

Unlike previous approaches, this setup uses the entire OFC spectrum without pre- filtering, simplifying the system and reducing cost. Stable locking is achieved with per-tone OFC powers as low as 1 nW, demonstrating the efficiency of the detection and control system. The low power

requirement enables multiple lasers to be locked to a single OFC via passive optical splitting.

From the experiment setup shown in Figure 4.2 we characterize the short-term stability measurement. Figure 4.3 below shows us phase noise of beat signal of one tunable laser lock to OFC (the read color) against two tunable lasers locked together (black color) using 2 PI^2 controller. We plot the locking two tunable lasers (black color) from phase noise result in Figure 3.8 to compare the two different scenarios. We can see that phase noise of one tunable laser lock to OFC has lower phase noise than 2 tunable lasers locked together.

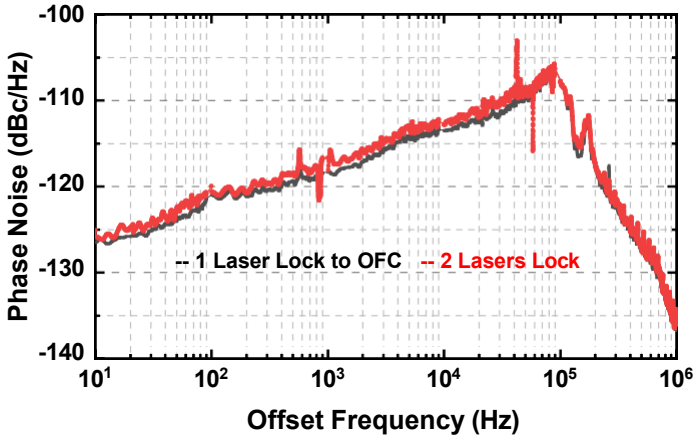

Figure. 4.3. Phase Noise of beat signal of one Tunable Laser lock to OFC against locking 2 Tunable Lasers using 2 PI^2 Controller.

4.3 Lock Acquisition

Lock acquisition represents a critical stage in the phase-locking experiment. In this case where a tunable laser locks to an OFC, the process requires investigating a suitable beat note, aligning the system to get maximum output, and determine the feedback loop to keep the stable beat signal. This section describes how to acquire a lock, how the system behaves both during and after acquisition, and how resilient the lock is in different scenario.

4.3.1 Beat Note Identification and Isolation

The first step in lock acquisition is the identification of a beat note between the tunable laser and the nearest comb tone.

- Beat Note Generation:
  - ✓ When the tunable laser wavelength is close to a comb line, interference produces a beat signal at the difference frequency.
  - ✓ The beat note appears as a spectral peak in the RF domain, typically around 30 MHz.

- Isolation Strategy:
    - ✓ A 50 MHz low-pass filter is used to suppress higher-order beat notes and noise from distant comb lines.
    - ✓ Then the beat signal is amplified and monitored to ensure it is stable.
- Optimization:
    - ✓ The beat signal amplitude is optimized by adjusting the polarization controller (PC).

4.3.2 Lock Acquisition Procedure

Once a stable beat note is identified, the feedback loop is engaged to acquire lock. Initial Conditions:

- The tunable laser is manually tuned to bring the beat note within the capture range of the phase detector.
    - ✓ The digital phase detector begins tracking the phase difference of the beating signal and the 30 MHz reference.
- Engaging the PI^4 Controller:
    - ✓ The controller applies corrections to the laser's phase actuator to minimize the phase error.
- Confirmation of Lock:
    - ✓ From RF Analyzer, we can observe the beat signal becomes more stable and narrower.
    - ✓ The frequency counter shows a steady reading with minimal drift.
    - ✓ The phase error signal stabilizes near zero.

4.3.3 Lock Stability and Robustness

After lock is acquired, the system is evaluated for its ability to maintain lock under various conditions.

- Power Fluctuations:
    - ✓ The system remains locked for long term even when the OFC power is as low as 1 nW per tone.
    - ✓ It shows that the system has high sensitivity and efficiency of the detection and control system.

4.3.4 Visual Indicators and Monitoring

- Spectrum Analyzer:
  - ✓ Used to visually confirm the presence and quality of the beat note.
  - ✓ Narrow linewidth and high SNR indicate successful locking.
- Frequency Counter:
  - ✓ Provides quantitative data on frequency stability.
  - ✓ Used to compute Allan deviation and long-term drift.

4.4 Controller Tuning and Optimization

The performance of a phase-locked loop (PLL) critically depends on the design and tuning of the controller. In this experiment, a PI^4 (Proportional–Double-Integrator) controller was implemented using a Red Pitaya FPGA platform [89] to achieve robust and low-noise locking of a telecom-grade tunable laser to an optical frequency comb (OFC).

4.4.1 Controller Architecture

- PI^2 Structure:
  - ✓ The controller consists of one PI^2 loops.
- PI^4 Structure:
  - ✓ The controller consists of two cascaded PI^2 loops, forming a PI^4 control system.
  - ✓ This structure enhances loop gain at low frequencies (for better long-term stability) while maintaining sufficient bandwidth to suppress high-frequency phase noise.
- Implementation Platform:
  - ✓ Red Pitaya STEMlab board with Xilinx Zynq 7010 SoC.
  - ✓ Real-time control loop operates at a sampling rate of 125 MS/s.

4.4.2 Tuning Methodology

The tuning process was iterative and guided by empirical testing.

- Initial Parameter Estimation:
    - ✓ Based on the loop dynamics from the two-laser setup.
    - ✓ Initial proportional and integral gains were scaled to account for the lower SNR and increased noise floor in the OFC case.
- Noise Optimization:
    - ✓ The integral gain was increased to suppress low-frequency drift.
    - ✓ A low-pass filter was added to the error signal path to reduce high-frequency noise coupling.

4.4.3 Differences from Two-Lasers Lock Case

Locking to an OFC introduced several new challenges that required modifications to the controller tuning strategy:

- Beat Note Ambiguity:
    - ✓ Multiple comb tones can produce beat signals within the detector bandwidth.
    - ✓ The controller had to be tuned to lock only to the dominant beat note (30 MHz), requiring careful filtering and gain shaping.
- Lower SNR:
    - ✓ The per-tone power from the OFC was significantly lower (~1–2 nW) compared to the two-lasers lock setup.
    - ✓ This necessitated higher loop gain and more aggressive noise filtering.
- Wider Dynamic Range:
    - ✓ The tunable laser had to track a broader range of frequencies due to the comb's spectral width.
    - ✓ The controller was tuned to maintain lock across a wider tuning range without instability.

4.5 Challenges and Mitigation Strategies

Locking a tunable laser to an optical frequency comb (OFC) is not like straightforward, as simple as locking two tunable lasers. Some difficulties that come from ultra-low power per comb tones, OFC complex spectrum structure, and the sensitivity of the system to environmental factors. This subsection point the major obstacles encountered and the strategies employed to overcome them.

4.5.1 Beat Note Ambiguity

Challenge:

- The OFC consists of thousands of closely spaced comb lines (250 MHz apart), all of which can interfere with the tunable laser to produce beat notes.

Mitigation Strategies:

- Low-pass filtering: A 50 MHz low-pass filter was deployed to isolate the desired beat signal (centered at 30 MHz) and suppress higher-frequency components.
- Manual tuning: The tunable laser was carefully adjusted to ensure that only one strong beat note appeared within the filter passband.

4.5.2 Low Signal-to-Noise Ratio (SNR)

Challenge:

- Individual comb tones have extremely low optical power (1–3 nW), resulting in weak beat signals that are easily buried in noise.
- Low SNR can degrade phase detection accuracy and destabilize the feedback loop.

Mitigation Strategies:

- High-sensitivity photodetector: A broadband, amplified photodetector with high responsivity (0.9 A/W) was used to maximize signal detection.
- Low-noise amplification: A Mini-Circuits ZFL-500HLN+ amplifier was installed to optimize the beat signal before processing.
- Optimized optical alignment: The polarization controller (PC) and variable optical attenuator (VOA) were adjusted to maximize interference contrast and beat signal strength.

4.5.3 Polarization Drift

Challenge:

- Changes in the environment and fiber birefringence can cause the polarization states of the OFC and tunable laser to drift over time.
- Misaligned polarization reduces beat signal amplitude and can cause lock loss.

Mitigation Strategies:

- Polarization controller: A manual PC was install before the coupler for allignment purpose.
- Periodic adjustment: For long term experiment, regular adjustment require to ensure maximum alignment.

4.5.4 Controller Stability and Loop Tuning

Challenge:

- The presence of multiple tones and low SNR made the control loop more prone to instability.
- Incorrect tuning could cause overshoot that lead to failure to acquire lock.

Mitigation Strategies:

- PI^4 controller: A higher-order controller was deployed to enhance loop stability and noise suppression.
- Empirical tuning: Controller parameters were iteratively adjusted based on response.

4.5.5 System Scalability

Challenge:

- Locking multiple lasers to the same OFC requires careful power budgeting.
- Adding another laser (multiple lasers) will reduces the available power per tone due to passive splitting.

Mitigation Strategies:

- Low power operation: Demonstrated stable locking with as little as 1 nW per tone, enabling multiple locks from a single OFC.
- Passive splitting: Optical splitters were used to distribute the OFC signal to multiple locking setups.

This chapter presented the experimental methodology for optical phase-locking a telecom- grade tunable laser to an OFC. Building on the benchmark from the two-laser locking configuration in Chapter 3, this setup introduced the complexity of locking to a multi-tones OFC while maintaining the goals of low cost, low power consumption, and high performance. These confirm that a single OFC can serve as a stable reference for multiple tunable lasers, enabling compact, comb-locked transmitter arrays and photonic synthesizers. The ability to operate with ultra-low per-tone power and without complex filtering makes this approach highly attractive for real-world applications.
Having established the feasibility and robustness of the OFC-locking system, the next chapter focuses on a detailed characterisation of its noise performance. Chapter 5 will explore both short-term and long-term stability metrics, including phase noise spectra, integrated jitter, frequency error, and Allan deviation. These analyses are essential for quantifying the system's precision and for benchmarking it against other state-of-the-art solutions.

Chapter 5

Noise Characterisation

In chapter 4, we demonstrated the successful phase-locking of a telecom-grade tunable laser to an optical frequency comb (OFC) using a low-cost, low-power setup. The system achieved stable locking with per-tone OFC powers as low as 1 nW, and maintained high performance across the C-band without the need for optical filtering. These confirmed that scalable, comb-locked laser systems are feasible for real-world use. This chapter focuses on a detailed analysis of the system's noise performance after showcasing the robustness and functionality of the locking mechanism. Characterising noise is essential for understanding the limitations of the phase-locking system and for benchmarking its suitability in precision- demanding applications such as coherent communications, frequency metrology, and Terahertz signal generation.

5.1 Locking Two Tunable Lasers

In this chapter, we present a comprehensive characterisation of both short-term and long- term noise. We begin by analysing the phase noise spectrum of the beat signal between the two lasers lock, as shown in figure 5.1., comparing different output power level of tunable laser 2 (Slave Laser) at the wavelength of 1550 nm. The experimental setup used for this measurement is shown in Figure 3.4.

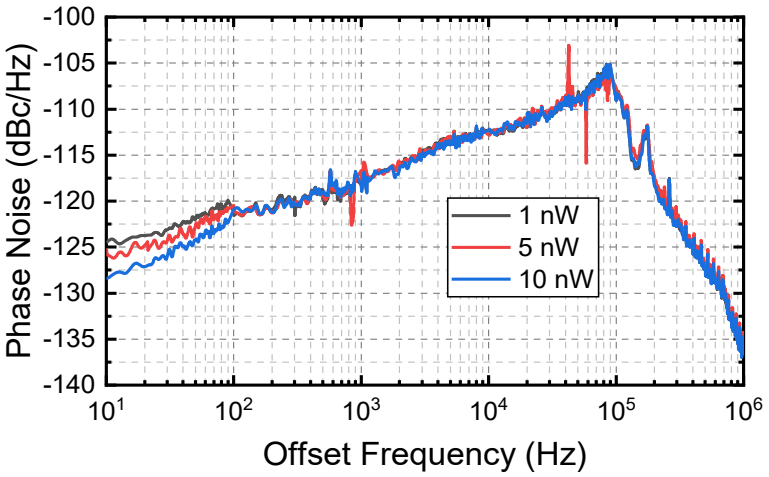

Figure. 5.1. Phase noise of beat signal between two tunable lasers with powers of 1 mW and 1-10 nW, respectively at the wavelength of 1550 nm.

The key variable in this experiment is the optical power of the second laser, which is varied from 1 nW to 10 nW at the photodetector input. This figure serves as a benchmark for evaluating the performance of the OFC-locking system under similar low-power conditions.

Key Observations from the Plot,

- High Offset Frequencies (>80 kHz) :

  ✓ Phase noise converges to the free-running laser noise floor.

  ✓ Feedback loop has limited influence in this region due to bandwidth constraints.

- Mid to Low Offset Frequencies (10 Hz – 80 kHz) :

  ✓ Phase noise decreases with decreasing offset frequency, as expected for a well-designed phase-locked loop.

  ✓ The PI^4 controller effectively suppresses phase noise in this region.

- Effect of Power Variation :

  - ✓ At 1 nW, the system still maintains lock with only a slight degradation in phase noise at very low frequencies (<100 Hz).
  - ✓ The difference between 1 nW and 10 nW is minimal, indicating robust locking performance even at ultra-low power.

Interpretation and Significance,

- Validation of Low-Power Operation :

  - ✓ Demonstrates that stable phase-locking is achievable with as little as 1 nW of optical power, which is critical for scalable systems using passive OFC splitting.

- Benchmark for OFC Locking :

  - ✓ This figure sets a performance baseline for later comparisons with the OFC-locking configuration.
  - ✓ It confirms that the OFC-locking system achieves comparable phase noise performance under the same power constraints.

- Environmental Sensitivity :

  - ✓ Minor fluctuations at low frequencies are attributed to environmental noise (e.g., thermal drift, mechanical vibrations), not to the locking mechanism itself.

Implications for System Design

- Detector and Amplifier Design :

  - ✓ The efficiency of the photodetector and RF amplification chain is confirmed by the system's capacity to recognize and process beat signals at 1 nW (slave laser).

- Controller Efficiency :

  ✓ The PI[4] controller provides sufficient loop gain and bandwidth to maintain lock and suppress noise, even under low-SNR conditions.

- Scalability :

  ✓ Since only 1 nW is needed per tone, a single OFC with 0.5 mW total power could theoretically support hundreds of simultaneous locks.

The key conclusion is that 1 nW (- 60 dBm) provides sufficient power for phase locking with minimum penalty on the performance.

5.2 A Tunable Laser Lock to OFC

Figure 5.2 below shows the phase noise spectrum of the beat signal between of one tunable laser to OFC, comparing different output power level of OFC per tone at the wavelength of 1550 nm. The experiment setup shown in figure 4.2.

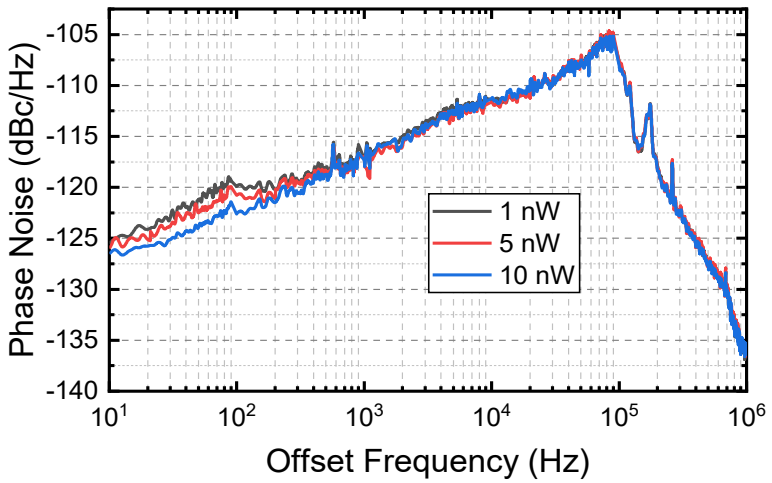

Figure. 5.2. Phase noise of the beat signal between a tunable laser (power of 1 mW) and OFC with per-tone power of 1-10 nW at the wavelength of 1550 nm.

Figure 5.2 presents the phase noise spectra of a tunable laser that is phase-locked to an OFC. We employed the same per-tone power level (1–10 nW) for this locking process, the same power used in the previous experiment shown in Figure 3.4, in which two tunable lasers were phase-locked to each other . In contrast to other research that usually uses tunable optical bandpass filters to separate particular comb tones, we used the full comb signal, which spans a 77-nm bandwidth, for photodetection. This method ensures that the photodetector receives the maximum per-tone OFC power while eliminating the requirement for tunable optical filters, which saves cost. Figure 5.2 is a direct counterpart to Figure 5.1, which showed the same analysis for a two- laser locking configuration. The objective is to show that, even in situations with extremely low power, the OFC-locking system performs on par with the two-lasers benchmark.

Key Observations from the Plot

- High Offset Frequencies (>80 kHz) :
  - ✓ Phase noise converges to the free-running laser noise floor, similar to Figure 5.
  - ✓ Indicates that the feedback loop is not active in this region due to bandwidth limitations.
- Mid to Low Offset Frequencies (10 Hz – 80 kHz) :
  - ✓ Phase noise decreases with decreasing offset frequency, showing effective loop suppression.
  - ✓ The curves for 1 nW, 5 nW, and 10 nW are nearly overlapping, indicating minimal performance degradation at lower power levels.
- Low-Frequency Region (<100 Hz) :
  - ✓ Slight fluctuations are observed, likely due to environmental noise (e.g., thermal drift, mechanical vibrations), not the locking mechanism.

TABLE 5.1. Comparison with Figure 5.1 (Two-Lasers Locking)

Feature	Figure 5.1 (Two Lasers)	Figure 5.2 (Laser to OFC)
Reference Signal	Second tunable laser	OFC comb tone
Beat Note Simplicity	Single tone	Multiple comb tones present
Filtering	Not required	No filtering used (full comb spectrum)
Phase Noise (1–10 nW)	Stable, low noise	Comparable performance
Locking Robustness	High	Equally high
Environmental Sensitivity	Slight low-frequency variation	Similar behavior

Despite the added complexity of multiple comb tones and the absence of optical filtering, the OFC-locking system performs on par with the two-laser configuration. It demonstrates that the locking performance is almost the same as that obtained when two lasers were locked to one another (as illustrated in Fig. 5.1). This result indicates that the simultaneous presence of numerous comb tones at the photodetector does not lead to any degradation in performance. Its resilience is confirmed by the results, which show that the full detection of all comb tones does not compromise the phase lock's stability or quality. This validates the robustness of the detection and control architecture and confirms that optical filtering is not necessary for stable locking at ultra-low power. By eliminating the need for extra filtering components, this technique streamlines the setup and makes use of every tone's full potential over the OFC bandwidth. Thus, without the hassles and costs of selective tone filtering, this work shows a practical and economical way to achieve high-quality laser locking.

Implications for System Design

- Scalability: Verifies that several lasers can be locked to one OFC without the need for filtering or high per-tone power.
- Cost Reduction: Eliminates the need for tunable optical filters, reducing system complexity and cost.
- Power Efficiency: Demonstrates that 1 nW per tone is sufficient for stable locking, enabling passive OFC splitting for multi-laser systems.

It provides critical evidence that the OFC-locking system is not only viable but also highly efficient and scalable.

We also investigated how the locking performance changes with wavelength, especially at different C-band locations. Figure 5.3 below evaluates the wavelength dependence of the phase-locking performance when a tunable laser is locked to an optical frequency comb (OFC). Specifically, it shows the phase noise spectra at three different wavelengths across the C-band:

- 1530 nm
- 1550 nm
- 1565 nm

These wavelengths were chosen to evaluate any possible performance variance brought on by variations in optical power throughout the spectrum.Each measurement was performed with the same per-tone OFC power of 1 nW, allowing a direct comparison of performance across the spectrum.

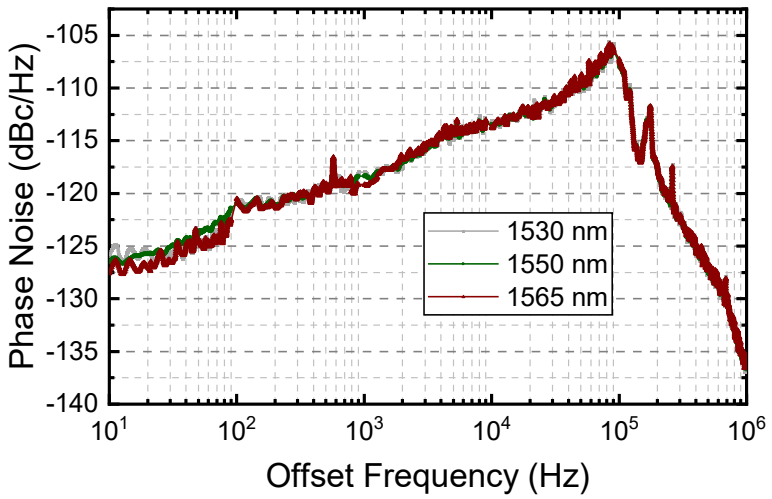

Figure. 5.3. Phase Noise of beat signal of locking tunable laser to the OFC at different wavelengths with relevant OFC power set to 1 nW.

Key Observations from the Plot

- Phase Noise Consistency:

  ✓ All three curves (1530, 1550, 1565 nm) show nearly identical phase noise behavior across the 10 Hz to 1 MHz offset range.

  ✓ This indicates that the locking performance is independent of wavelength, even when the comb tone power varies significantly.

- Low-Frequency Region (<100 Hz) :

  ✓ Slight fluctuations are visible, likely due to environmental noise (e.g., thermal drift), not due to the locking mechanism.

- High Offset Frequencies (>80 kHz) :

  ✓ Phase noise converges to the free-running laser noise floor, as expected.

Interpretation and Significance

- Spectral Robustness:
  - ✓ The system maintains high locking performance across the C-band, despite a 5.3 dB variation in comb tone power (from 1.1 nW to 3.7 nW).
  - ✓ This confirms the robustness of the detection and control system to spectral non-uniformity in the OFC.
- No Need for Power Equalization :
  - ✓ Unlike systems that require flat comb spectra or optical amplification, this setup works reliably without any power equalization or filtering.
- Practical Implications:
  - ✓ Enables use of low-cost, compact OFCs with non-uniform spectra.
  - ✓ Supports flexible wavelength allocation in DWDM systems and photonic THz generation.

The findings show that the phase noise performance is constant at 1530 nm and all other investigated wavelengths. Interestingly, compared to the comb tones at longer wavelengths, such as 1575 nm, the power of the matching comb tone at 1530 nm is much lower. Phase-locking applications, where consistent tone power across the spectrum is necessary for ensuring optimal stability and noise reduction, are complicated by the varying power levels of comb tones. With phase noise levels comparable to those seen at higher- power wavelengths, our phase-locking setup performs well even if the power at 1530 nm is reduced. The locking technique is durable despite this lower power level at 1530 nm since it continues functioning similarly to the other wavelengths in phase noise. It provides strong evidence that the OFC-locking system is spectrally agnostic, making it ideal for real-world applications where comb tone power varies across the spectrum.

In this work, we concentrate on a thorough description of our configuration, which uses a per-tone OFC power of 1 nW to phase-lock a tunable laser to an OFC. The objective is to evaluate the impacts of various control schemes on phase noise performance, with a particular comparison of the effects of PI^2 and PI^4 controllers as shown in figure 5.4. The experiment setup is depicted in Fig. 4.1.

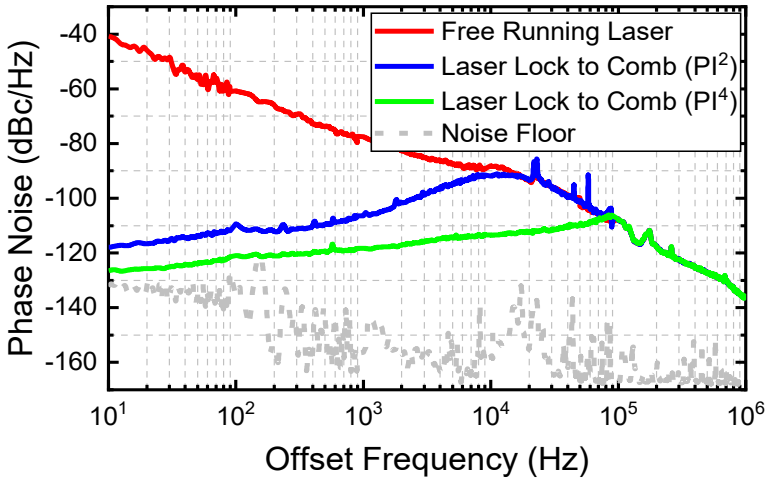

Figure. 5.4. Phase noise of the beat signal between a tunable laser (power of 1 mW) and OFC with per-tone power of 1 nW at the wavelength of 1550 nm for free-running laser (blue), when phaselocked using one double- integrator (PI^2, blue), and using two double-integrators (PI^4, green). Measured noise floor is also shown (grey, dashed).

Figure 5.4 provides a comparative analysis of the phase noise performance of a tunable laser locked to an optical frequency comb (OFC) using two different feedback controller configurations:

- PI^2 controller (single proportional–double-integrator loop)

- PI^4 controller (two cascaded PI^2 loops)

It also includes the free-running laser phase noise and the measurement noise floor, offering a complete view of the system's noise suppression capabilities. The noise floor of the digital phase detector measurement scheme can be measured by connecting the two input ports of digital phase detector with two similar reference signals, this baseline evaluates the PI^2 and PI^4 controllers' suppression capabilities and shows the lowest detectable phase noise. We found the best settings for both PI^2 and PI^4 controllers by adjusting each controller's characteristics to produce the best phase noise suppression, these are compiled in Tables 5.2 and 5.3.

TABLE 5.2 Optimum parameters for single PI^2.

Quantity	Value
Proportional gain, *kp*	7.3
Integrator gain *ki*	1.74×10^4
2nd Integrator gain *kii*	1.66×10^3

TABLE 5.3 Optimum parameters for two PI^2 (PI^4)

Quantity	First PI^2	Second PI^2
Proportional gain, *kp*	2.6	12.5
Integator gain, *ki*	1.2×10^6	1.38×10^3
2^{nd} Integrator gain *kii*	3.02×10^2	2.34×10^4

Key Observations from the Plot

- Free-Running Laser (Red Curve)
  - ✓ Exhibits high phase noise across the spectrum.
  - ✓ Serves as a baseline to show the effectiveness of the locking system.
- PI^2 Controller (Blue Curve)
  - ✓ Provides significant noise suppression below ~20 kHz.
  - ✓ Phase noise drops by ~78 dB at 10 Hz offset compared to the free-running laser.
  - ✓ However, suppression is limited at mid-range frequencies (1–10 kHz).
- PI^4 Controller (Green Curve)
  - ✓ Offers superior noise suppression across the entire offset frequency range.

- ✓ Achieves:
  - ~13 dB improvement at 1 kHz offset.
  - ~20 dB improvement at 10 kHz offset.
- ✓ Phase noise at 10 Hz approaches the measurement noise floor, indicating near- optimal performance.

- Measurement Noise Floor (Grey Dashed Line)
  - ✓ Represents the lowest detectable phase noise in the system.
  - ✓ PI^4 performance nearly reaches this floor at low offset frequencies.

Interpretation and Significance

- Loop Bandwidth:
  - ✓ PI^2: ~20 kHz.
  - ✓ PI^4: ~100 kHz.
  - ✓ The control bandwidth is greatly increased by the PI^4 controller, improving mid-frequency noise suppression.
- Noise Suppression:
  - ✓ PI^4 attains better and wider suppression, particularly in the critical 1–10 kHz range, which is important for applications requiring high spectral purity.

- System Optimization:

  - ✓ The PI^4 controller is more effective at utilizing the available modulation bandwidth of the laser (~100 kHz).
  - ✓ Shows the benefits of digital locking systems that use a higher-order control loop.

Practical Implications

- Precision Applications:

  - ✓ The PI^4 controller is better suited for applications like coherent communications, frequency metrology, and THz generation, where low phase noise is critical.
- Hardware Efficiency:

  - ✓ Although the current PI^4 implementation uses two parallel PI^2 loops, future FPGA reprogramming could consolidate this into a single optimized loop, improving scalability.

The findings show that the PI^4 controller greatly improves noise suppression and control bandwidth. In particular, the PI^4 controller increases the locking bandwidth from 20 kHz (when using PI^2) to 100 kHz, which enables more efficient laser control across a wider frequency range. This bandwidth expansion makes better phase noise suppression at low offset frequencies, where it is most important for preserving a stable phase lock, possible. Compared to the PI^2 controller, the PI^4 controller exhibits reductions of 13 dB and 20 dB in phase noise at offset frequencies of 1 kHz and 10 kHz from the carrier. Both controllers suppress phase noise at an offset frequency of 10 Hz, with reductions of 78 dB to 87 dB compared to the free-running laser. The configuration is functioning close to the lowest noise levels that our system can detect, as demonstrated by the fact that the phase noise at 10 Hz acquired with the PI^4 controller almost matches our measurement noise floor. It provides compelling evidence of the performance gains achieved through advanced control loop design.

The performance of the phase-locking system was assessed by integrating the phase-noise spectra, rather than time-domain jitter, to obtain the RMS phase deviation for both the PI^2 and PI^4 controllers. The results are illustrated in figure 5.5. The figure presents a quantitative comparison of integrated phase noise jitter for a tunable laser phase-locked to an OFC using those two different feedback control strategies. The graphic shows how the total phase jitter, a crucial criterion for assessing the locked laser's spectral purity and stability, is impacted by the controller architecture selection. Integrated Phase noise is an important parameter, reflecting the cumulative impact of phase noise across the frequency range, which directly affects the stability and accuracy of the laser locking system.

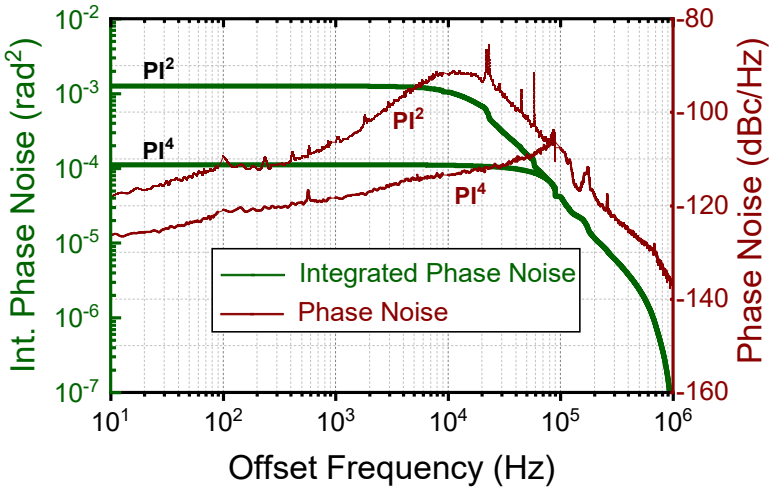

Figure. 5.5. Phase noise jitter calculated from the measured phase noise of OFC-locked tunable laser (with per-tone power of 1 nW) when locked using PI^2 and PI^4 feedback controller.

For each controller, we integrated phase noise over the whole measurement bandwidth (10 Hz to 1 MHz) in order to quantify the resulting jitter. While the PI^4 controller demonstrated a significantly lower jitter of 10 mrad, the PI^2 controller generated a jitter of 35 mrad. With around three times less jitter than the PI^2, the observed difference highlights the PI^4 controller's improved noise suppression performance.

Given the limitations of the system, such as its low-cost electronic components and bandwidth limitations, the results are notable. Despite these drawbacks, our configuration

achieves jitter reductions of more than 100 times above those reported in previous research, such as [91]. This notable improvement demonstrates how well the PI4 controller works to lower phase noise and jitter even in a setting with limited resources and bandwidth.

According to the integration results, a PI^4 controller provides better jitter performance, making it the best choice for applications that need to have low levels of phase noise and jitter. This setup reduces complexity and expense while establishing a steady and dependable phase lock. It is appropriate for a wide range of demanding applications that need for excellent stability, little noise, and effective use of resources.

Long-term Stability

We evaluated the long-term stability of our phase-locking setup by conducting measurements over prolonged observation periods, explicitly focusing on timescales more significant than 100 microseconds and extending to 1 second. For long-term applications, stability is essential, and the observation times correspond to low frequencies of 10 kHz and 1 Hz, respectively. To evaluate the stability of the system over different timescales, we used a frequency counter (Keysight 53230A).

At a sampling rate of one second, the primary goal was to evaluate how frequency error changed over time. In order to identify any drifts or variations and to confirm the stability and robustness of the locking system, this measurement was carried out for a period of ten hours. The frequency error data for the PI^2 and PI^4 controllers are shown in Figure 5.6.

The findings demonstrate that the PI^4 controller offers markedly improved long-term stability in comparison to the PI^2. The PI^4 controller demonstrated a peak-to-peak frequency error consistently within ±0.01 Hz, indicating a stability approximately five times greater than that of the PI^2 controller. The significant decrease in frequency error suggests that the PI^4 controller provides a notable enhancement in stability, even during extended observation periods.

The attained stability is noteworthy when compared to earlier findings. The frequency variation with the PI^4 controller was approximately 100 times lower than that reported in [91], demonstrating the

efficacy of our method in sustaining accurate frequency control over prolonged periods. The significant stability of the PI^4 controller highlights its appropriateness for applications requiring durable, long-term locking with minimal frequency drift, rendering it an effective solution for high-precision optical systems.

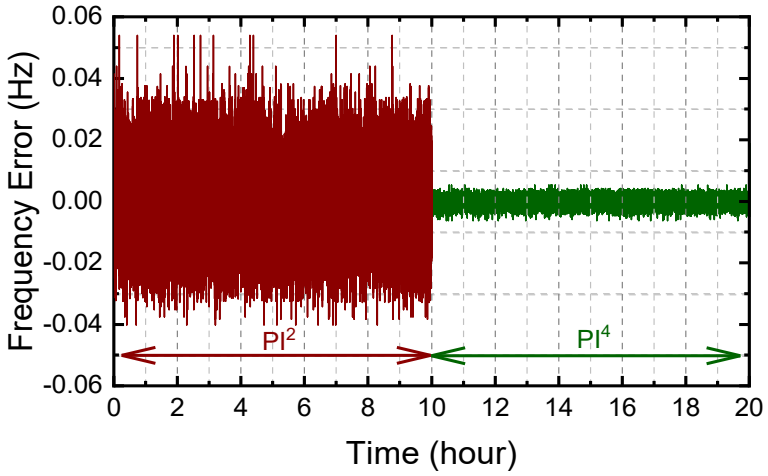

Figure. 5.6. Frequency error of OFC-laser beat signal with one double-integrator (PI^2) and two double-integrators (PI^4) using 1 s gate time, measured over 10 hours.

By computing the Allan deviation from the frequency error data shown in Fig. 5.6, we evaluated the stability of our phase-locking configuration. A common statistic for assessing frequency stability over a range of averaging intervals is Allan deviation, which provides information on performance differences over longer observation periods. We augmented this data with further measurements acquired at a reduced gating time of 4 microseconds (μs) to broaden the observation range. This enabled an analysis of stability over a wide range of averaging times, from 100 μs to 1000 seconds, as illustrated in Fig. 5.7.

The Allan deviation data show distinct patterns over a range of periods. With τ being the average time, the Allan deviation has a slope that is inversely proportional to τ in the range of 100 microseconds to 100 miliseconds. According to the inverse connection, the system shows notable stability across shorter durations, which is in line with the PI^4 controller's increased control bandwidth. The slope starts to drop at observation times longer than 100 miliseconds, most likely because of low-frequency drift in the configuration. Variations in temperature or slow changes in the setup

elements may be the cause of this drift, which can impact frequency stability over extended periods of time.

According to this analysis, the PI^4 controller exhibits noticeably higher stability than the PI^2 controller over all averaging times, as seen by Allan deviation values that are roughly an order of magnitude lower. With an averaging time of 1 second, the PI^4-controlled setup attains a stability level of approximately 2×10^{-14}. The achieved stability confirms that the PI^4 controller effectively reduces frequency variation , making it especially suitable for precision applications that require reliable performance across short and long observation times.

The Allan deviation analysis highlights the superiority of the PI^4 controller in phase-locking applications. The PI^4 controller improves overall stability and reliability by maintaining lower deviation across all timescales, resulting in minimal drift and consistent performance over extended periods. The stability of high-precision systems is essential for consistent frequency control, which is necessary to maintain signal integrity and reduce error.

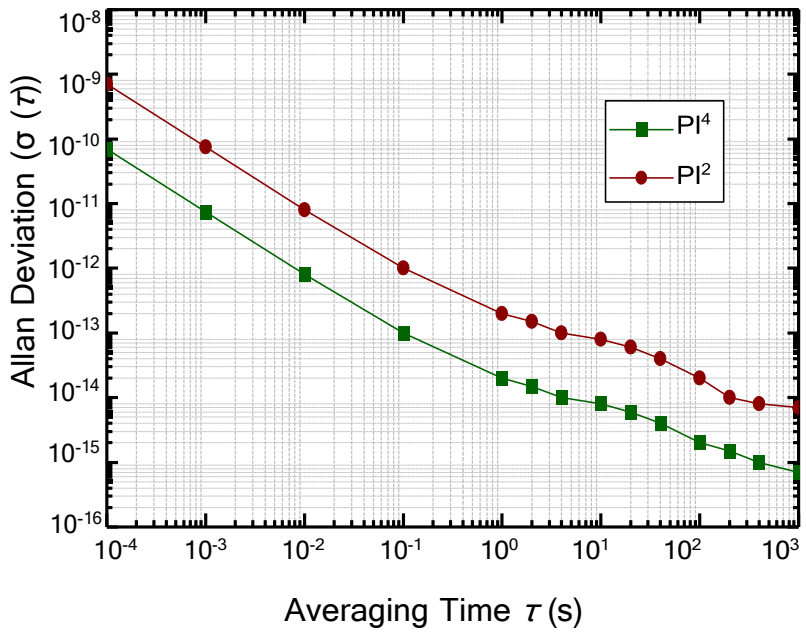

Figure. 5.7. Allan deviation calculated from the frequency counter data when a tunable laser is locked to the OFC using two double-integrators (PI^4) and one double-integrator (PI^2), normalized to the laser carrier frequency (192 THz).

5.3 Discussion

This study primarily characterizes the performance of a single tunable laser phase-locked to an OFC. Through passive signal splitting, this method's potential scalability enables the simultaneous locking of many lasers to the same OFC. Multiple lasers can be locked to different OFC spectrum regions with this configuration. As mentioned in [92], these locked lasers can produce extremely stable radio frequency signals across a wide frequency range through subsequent photomixing.

It is possible to generate an RF signal up to 4.5 THz by using two C-band tunable lasers. Moreover, the range is increased to about 9 THz by combining an L-band laser with a single C-band tunable laser. The main benefit of locking both lasers to the OFC is the substantial reduction in phase noise of the generated beat signal, which is considerably lower than that produced by two independent lasers.

To estimate the performance attainable in a multi-laser configuration, we assume that each laser is phase-locked to its corresponding comb tone. The Allan deviation data in Fig. 5.7 can be scaled to get the fractional frequency stability for this locking configuration. In order to account for the dual-laser arrangement, an extra factor of two is added to the scaling, which is carried out in relation to the frequency gap between the two locked lasers. Figure 5.8 presents the results, illustrating fractional frequency instability across various laser frequency spacings with an average time of 1 second.

The fractional frequency instability demonstrates improvement as the frequency spacing between the lasers increases. This enhancement arises from the fact that, although the locking stability is maintained, an increased frequency difference between the lasers leads to reduced relative instability. We also plotted the fractional frequency instability of our optical frequency comb, constrained by its RF reference (Timetech 5.10), which demonstrates a stability of 5×10^{-13} at a 1-second averaging time. The stability of the beat frequency between the two locked lasers is lower than that of the OFC, suggesting that the phase-locking performance of the lasers is adequate and not constrained by the quality of the OFC reference.

However, if an OFC were utilized with a lower-quality radio frequency reference (e.g., exhibiting instability in the 10^{-11} range at a 1-second averaging time), the stability of the beat frequency would be constrained by the OFC itself rather than the laser phase-locking configuration. This scenario is characteristic of optical fibre communications utilizing standard crystal oscillators, as opposed to the high-quality laboratory-grade reference employed in this context. The performance of the OFC serves as the primary limiting factor, with our laser locking contributing minimally to overall stability. This confirms the sufficiency of our laser phase-locking performance for precision applications.

Additionally, Fig. 5.8 displays fractional frequency instability values from multiple sources, as adapted from [93]. While higher quality OFCs may yield enhanced outcomes [94], our method exhibits up to two orders of magnitude improved fractional frequency instability relative to photomixing with two continuous-wave (CW) lasers [95], [96], [97] for frequencies exceeding 0.1 THz. This method produces results that are similar to those achieved through photomixing with microcombs [98], [99] and quantum cascade lasers [100], [101], [102]. Nonetheless, a significant benefit of our method is its tunability, which is absent in both microcomb and quantum cascade laser techniques.

With remarkable fractional frequency stability and a significant decrease in phase noise, the laser to OFC-locking technology produces stable, low-noise radio frequency signals throughout a broad frequency range. This system is appropriate for high-precision applications that require both stability and flexibility in frequency generation because it offers an appealing combination of performance and tunability.

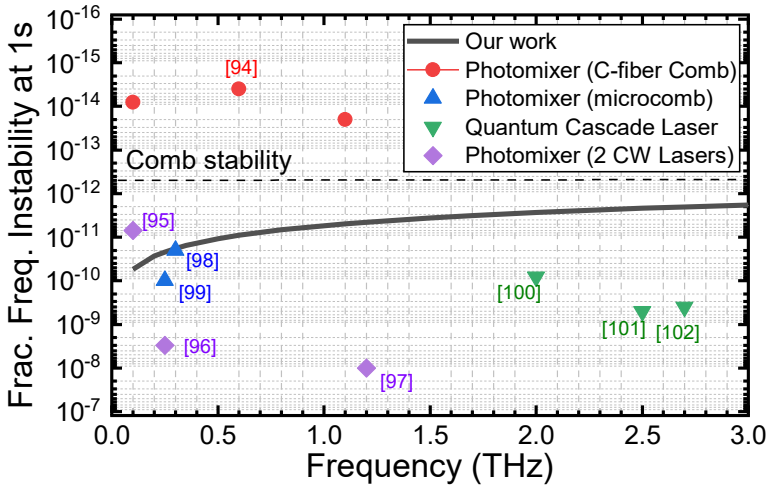

Figure.5.8. Fractional frequency instability of the beat signal at 1 s averaging times for various beat frequencies expected from our system and its comparison with the state-of-the art Terahertz sources (adopted from [94]).

This chapter provided a comprehensive analysis of the noise characterisation of the phase- locked tunable laser system, both short-term and long-term stability.

The key findings are as follows:

- **Short-Term Stability**:

  Using a PI^4 controller greatly enhanced noise suppression over a wide frequency range, according to phase noise measurements. Over a bandwidth of 10 Hz to 1 MHz, the system achieved an integrated phase jitter of roughly 10 mrad., with phase noise levels approaching the measurement noise floor at low offset frequencies.

- **Long-Term Stability**:

  Frequency error measurements over a 10-hour period showed peak-to-peak variations within ±0.01 Hz when using the PI^4 controller—five times better than with a PI^2 controller. Allan deviation analysis confirmed a fractional frequency stability of 2

  $\times 10^{-14}$ at 1-second averaging time, with performance maintained across a wide range of integration times.

- **Stable Locking at 1 nW**

  Minimum power: Stable locking was achieved with as low as 0.5 nW of optical power reaching the photodetector.

  Performance: Phase noise and jitter remained nearly identical to those observed at higher powers (5–10 nW), especially above 100 Hz offset frequency.

  Implication: This confirms that the system is highly efficient in extracting and processing the beat signal, even under low-SNR conditions.

- **No Optical Filtering Required**

  The entire OFC spectrum (77 nm bandwidth) was used without any tunable bandpass filters.

  Advantage: This approach maximizes the per-tone power reaching the detector and eliminates the need for costly and bulky optical filtering components.

  Observation: Despite the presence of multiple comb tones, no degradation in locking performance was observed, indicating effective suppression of unwanted beat signals via low-pass filtering and digital controller feedback.

- **Robustness**:

  The system showed resilience to spectral non-uniformity and environmental changes by maintaining consistent performance across a range of wavelengths and OFC tone powers.

  In conventional OFC locking systems, achieving a stable phase lock often requires high per-tone optical power (milliwatt typically) and the use of tunable optical filters to isolate individual comb lines. These requirements increase system complexity, cost, and power consumption, factors that limit scalability and practical deployment.

This work demonstrates that stable phase-locking can be achieved. This breakthrough enables:

- Passive splitting of the OFC to lock multiple lasers simultaneously.
- Simplified optical architecture, reducing component count and alignment sensitivity.
- Lower power budget, making the system suitable for compact and integrated platforms.

These findings demonstrate that the system sustains spectrum purity and frequency stability over time in addition to achieving reliable phase-locking. This technique is very appealing for scalable, real-world deployment due to its robust noise performance, low optical power requirements, and inexpensive hardware. With the system's performance now fully characterised, the final chapter of this thesis will summarise the key contributions of this research and outline potential directions for future work. Chapter 6 will reflect on the broader implications of this work and explore how the developed techniques can be extended to support emerging applications in photonics and beyond.

Chapter 6

6.1 Conclusions

This thesis has presented the development, implementation, and characterization of a practical system for phase-locking telecom-grade tunable lasers to an optical frequency comb (OFC). The work addresses a critical need for stable, tunable, and cost-effective laser sources in applications such as Terahertz signal generation, spectroscopy.

The key contributions and findings of this research are summarized as follows :

- **Low-Power Phase Locking**

  Nanowatt OFC power per tone was used to demonstrate a reliable phase-locking method, and locking was successful at power levels as low as 1 nW. Compared to earlier systems that needed considerably greater power levels and frequently required optical amplification, this is a significant reduction. This enables the use of a single OFC to phase-lock multiple lasers via passive optical splitting, simple optical splitter (e.g., 1×N couplers), avoiding the need for active or tunable components, significantly enhancing scalability and reducing system cost. The low power requirement per laser means the system can scale to many lasers without increasing the OFC power or adding amplifiers. Eliminating the need for active splitter, tunable optical filters and high-power OFCs reduces both hardware complexity and cost. The system uses telecom-grade tunable lasers and low-cost FPGA-based controllers (e.g., Red Pitaya), making it practical for commercial deployment.

- **Controller Design and Optimization**

  Compared to laboratory-grade lasers, tunable lasers, particularly telecom-grade ones, have a smaller control bandwidth and more phase noise. The loop bandwidth of a typical PI^2 controller was sufficient to suppress this noise. By including an additional integrator, the PI^4 controller enhances phase noise suppression and frequency stability by raising the loop gain at low frequencies. Using a low-cost FPGA platform (Red Pitaya), a new PI^4 (proportional–double-integrator) feedback controller was put into practice. Phase noise suppression and frequency stability were enhanced by the PI^4 configuration's fivefold increase in loop bandwidth over the traditional PI^2 controller.

- **Performance Characterization**

  Achieved 10 milliradians (mrad) of integrated phase jitter over the 10 Hz–1 MHz range using the PI^4 controller. This is a strong indicator of low phase fluctuations and high coherence. The system showed suppression of phase noise below 100 kHz offset frequency. At 10 Hz offset, the PI^4 controller achieved > 70 dB suppression compared to the free-running laser. The feedback loop bandwidth was extended to ~100 kHz using the PI^4 controller, compared to ~20 kHz with PI^2. Stable locking and consistent phase noise performance were demonstrated across the entire C- band (1530–1565 nm), even when comb tone powers varied (e.g., 1.1 nW at 1530 nm vs. 3.7 nW at 1565 nm).

  Peak-to-peak frequency error over 10 hours was ±0.01 Hz with the PI^4 controller. This is a fivefold improvement over the PI^2 controller (±0.05 Hz). At 1-second averaging time, the system achieved a fractional frequency stability of 2×10^{-14}. This level of stability is suitable for high-precision applications like THz generation and optical metrology.

- **Scalability and Field Deployable**

  The system is very feasible for real-world deployment because it was developed with minimum optical hardware and commonly available telecom components. The elimination of tunable optical filters and the use of low-bandwidth electronics further reduce complexity and cost, but need rack-mounted OFC.

- **Application Potential**

  Applications needing numerous coherent sources, including comb-locked DWDM transmitters and photonic THz generation, are ideally suited for the technology. Its adaptability is demonstrated by the fact that lasers can be locked across the whole C-band with little loss in performance.

All things considered, our study paves the way for a broader use of OFC-based systems beyond conventional metrology by demonstrating that high-performance, comb-locked tunable lasers may be realized using inexpensive, scalable, and power-efficient designs.

6.2 Future Work

While the results presented in this thesis are promising, several avenues for future research and development remain :

- **FPGA Integration and Optimization**

  The current implementation of the PI^4 controller uses two parallel PI^2 controllers. These two controllers process the same input signal independently and their outputs are combined to simulate the behavior of a PI^4 controller. While effective, this approach is resource-intensive and not optimal for scaling. Future work could involve reprogramming the FPGA to implement a true single-input (the error signal from the phase detector), and single-output PI^4 controller (the control signal to the laser), Integrated double integrators and proportional gain in a single control loop, thereby freeing up resources to lock multiple lasers simultaneously on a single board.

- **Multi-Laser Locking Demonstration**

  A natural extension of this work is the experimental demonstration of simultaneous phase-locking of multiple tunable lasers to different OFC tones. This would validate the scalability of the system and its suitability for multi-channel applications, like Dense Wavelength Division Multiplexing (DWDM), Photonic Terahertz generation, Multi-channel coherent communication systems, spectroscopy and sensing with multiple coherent sources.

- **Extension to Other Bands**

  While this work focused on the C-band, extending the approach to the L-band could broaden the range of applications, particularly in terahertz, spectroscopy and sensing.

- **Integration with Photonic THz Systems**

  High-purity THz signal synthesis could be experimentally shown by integrating the system with photomixing method. Important benchmarks would be provided by performance comparisons with other THz sources, such as microcombs and quantum cascade lasers.

- **Improved OFC Sources**

  As the system is designed to work with low-power, non-flat OFCs, future work could explore the use of compact, integrated OFC sources with higher tone spacing (e.g., GHz-level) to simplify tone selection and improve robustness.

- **Environmental Robustness**

  To determine whether the system is suitable for field deployment, more research might examine how well it performs in various environmental conditions (such as temperature and mechanical vibrations).

References

[1] A. L. Schawlow and C. H. Townes, “Infrared and Optical Masers,” *Physical Review*, vol. 112, no. 6, pp. 1940–1949, Dec. 1958, doi: 10.1103/PhysRev.112.1940.

[2] T. H. MAIMAN, “Stimulated Optical Radiation in Ruby,” *Nature*, vol. 187, no. 4736, pp. 493–494, Aug. 1960, doi: 10.1038/187493a0.

[3] R. N. Hall, G. E. Fenner, J. D. Kingsley, T. J. Soltys, and R. O. Carlson, “Coherent Light Emission From GaAs Junctions,” *Phys Rev Lett*, vol. 9, no. 9, pp. 366–368, Nov. 1962, doi: 10.1103/PhysRevLett.9.366.

[4] J. Fuchsberger, T. P. Letsou, D. Kazakov, R. Szedlak, F. Capasso, and B. Schwarz, “Continuously and widely tunable semiconductor ring lasers,” *Optica*, vol. 12, no. 7, p. 985, Jul. 2025, doi: 10.1364/OPTICA.559884..

[5] S. A. Diddams, “The evolving optical frequency comb [Invited],” *Journal of the Optical Society of America B*, vol. 27, no. 11, p. B51, Nov. 2010, doi: 10.1364/JOSAB.27.000B51.

[6] V. Torres-Company et al., “Laser Frequency Combs for Coherent Optical Communications,” *Journal of Lightwave Technology*, vol. 37, no. 7, pp. 1663–1670, Apr. 2019, doi: 10.1109/JLT.2019.2894170.

[7] J. H. Wong *et al.*, “Photonic Generation of Frequency-Tunable Microwave Signals Using an Array of Uniformly Spaced Optical Combs,” *Journal of Lightwave Technology*, vol. 30, no. 19, pp. 3164–3172, Oct. 2012, doi: 10.1109/JLT.2012.2215008.

[8] Z. Feng, A. Tourigny-Plante, J. Vojtěch, J. Genest, D. J. Richardson, and R. Slavík, “Comb-locked telecom-grade tunable laser using a low-cost FPGA-based lockbox,” in *Conference on Lasers and Electro-Optics*, Washington, D.C.: Optica Publishing Group, 2021, p. STu1J.4. doi: 10.1364/CLEO_SI.2021.STu1J.4.

[9] Z. Liu and R. Slavík, “Optical Injection Locking: From Principle to Applications,” *Journal of Lightwave Technology*, vol. 38, no. 1, pp. 43–59, Jan. 2020, doi: 10.1109/JLT.2019.2945718.

[10] A. Tourigny-Plante, V. Michaud-Belleau, N. Bourbeau Hébert, H. Bergeron, J. Genest, and J.-D. Deschênes, “An open and flexible digital phase-locked loop for optical metrology,” *Review of Scientific Instruments*, vol. 89, no. 9, pp. 1–5, Sep. 2018, doi: 10.1063/1.5039344.

[11] R. Adler, “A Study of Locking Phenomena in Oscillators,” *Proceedings of the IRE*, vol. 34, no. 6, pp. 351–357, Jun. 1946, doi: 10.1109/JRPROC.1946.229930.

[12] J.-L. Lachambre, P. Lavigne, G. Otis, and M. Noel, “Injection locking and mode selection in TEA-CO_2 laser oscillators,” *IEEE J Quantum Electron*, vol. 12, no. 12, pp. 756–764, Dec. 1976, doi: 10.1109/JQE.1976.1069085.

[13] J. Goldhar, J. Dickie, L. P. Bradley, and L. D. Pleasance, “Injection locking of a xenon fluoride laser,” *Appl Phys Lett*, vol. 31, no. 10, pp. 677–679, Nov. 1977, doi: 10.1063/1.89501.

[14] S. Blit, U. Ganiel, and D. Treves, “A tunable, single mode, injection-locked flashlamp pumped dye laser,” *Applied Physics*, vol. 12, no. 1, pp. 69–74, Jan. 1977, doi: 10.1007/BF00900070.

[15] S. Kobayashi and T. Kimura, “Coherence of injection phase-locked AlGaAs semiconductor laser,” *Electron Lett*, vol. 16, no. 17, pp. 668–670, Aug. 1980, doi: 10.1049/el:19800474.

[16] S. Kobayashi and T. Kimura, “Injection locking characteristics of an AlGaAs semiconductor laser,” *IEEE J Quantum Electron*, vol. 16, no. 9, pp. 915–917, Sep. 1980, doi: 10.1109/JQE.1980.1070595.

[17] L. Goldberg, H. F. Taylor, and J. F. Weller, “FM sideband injection locking of diode lasers,” *Electron Lett*, vol. 18, no. 23, pp. 1019–1020, Nov. 1982, doi: 10.1049/el:19820698.

[18] K. Otsuka and S. Tarucha, “Theoretical studies on injection locking and injection-induced modulation of laser diodes,” *IEEE J Quantum Electron*, vol. 17, no. 8, pp. 1515–1521, Aug. 1981, doi: 10.1109/JQE.1981.1071296.

[19] R. Lang, “Injection locking properties of a semiconductor laser,” *IEEE J Quantum Electron*, vol. 18, no. 6, pp. 976–983, Jun. 1982, doi: 10.1109/JQE.1982.1071632.

[20] C. Henry, “Theory of the phase noise and power spectrum of a single mode injection laser,” *IEEE J Quantum Electron*, vol. 19, no. 9, pp. 1391–1397, Sep. 1983, doi: 10.1109/JQE.1983.1072058.

[21] P. Gallion and G. Debarge, “Influence of amplitude-phase coupling on the injection locking bandwidth of a semiconductor laser,” *Electron Lett*, vol. 21, no. 7, pp. 264–266, Mar. 1985, doi: 10.1049/el:19850188.

[22] K. Kobayashi, H. Nishimoto, and R. Lang, “Experimental observation of asymmetric detuning characteristics in semiconductor laser injection locking,” *Electron Lett*, vol. 18, no. 2, pp. 54–56, Jan. 1982, doi: 10.1049/el:19820038.

[23] G. Großkopf and L. Küller, “Experimental study of stability properties of injection-locked InGaAsP/InP laser diodes,” *Opt Quantum Electron*, vol. 17, no. 4, pp. 269–275, Jul. 1985, doi: 10.1007/BF00620452.

[24] N. Olsson *et al.*, “Chirp-free transmission over 82.5 km of single mode fibers at 2 Gbit/s with injection locked DFB semiconductor lasers,” *Journal of Lightwave Technology*, vol. 3, no. 1, pp. 63–67, 1985, doi: 10.1109/JLT.1985.1074146.

[25] K. Kikuchi and C. E. Zah, “Spectral, phase noise and phase modulation characteristics of AM sideband injection-locked semiconductor lasers,” *Electron Lett*, vol. 23, no. 9, pp. 437–439, Apr. 1987, doi: 10.1049/el:19870315.

[26] R. Hui, A. D’Ottavi, A. Mecozzi, and P. Spano, “Injection locking in distributed feedback semiconductor lasers,” *IEEE J Quantum Electron*, vol. 27, no. 6, pp. 1688–1695, Jun. 1991, doi: 10.1109/3.89994.

[27] T. Ogawa, Y. Ida, and K. Hayashi, “Experimental determination of gain compression factors of a DFB laser in the presence of TM light injection,” *IEEE Photonics Technology Letters*, vol. 4, no. 4, pp. 345–348, Apr. 1992, doi: 10.1109/68.127208.

[28] F. Mogensen, H. Olesen, and G. Jacobsen, “Locking conditions and stability properties for a semiconductor laser with external light injection,” *IEEE J Quantum Electron*, vol. 21, no. 7, pp. 784–793, Jul. 1985, doi: 10.1109/JQE.1985.1072760.

[29] C. Henry, N. Olsson, and N. Dutta, “Locking range and stability of injection locked 1.54 μm InGaAsp semiconductor lasers,” *IEEE J Quantum Electron*, vol. 21, no. 8, pp. 1152–1156, Aug. 1985, doi: 10.1109/JQE.1985.1072787.

[30] P. Spano, S. Piazzolla, and M. Tamburrini, “Frequency and intensity noise in injection-locked semiconductor lasers: Theory and experiments,” *IEEE J Quantum Electron*, vol. 22, no. 3, pp. 427–435, Mar. 1986, doi: 10.1109/JQE.1986.1072982.

[31] I. Petitbon, P. Gallion, G. Debarge, and C. Chabran, “Locking bandwidth and relaxation oscillations of an injection-locked semiconductor laser,” *IEEE J Quantum Electron*, vol. 24, no. 2, pp. 148–154, Feb. 1988, doi: 10.1109/3.108.

[32] O. Lidoyne, P. Gallion, C. Chabran, and G. Debarge, “Locking range, phase noise and power spectrum of an injection-locked semiconductor laser,” *IEE Proceedings J Optoelectronics*, vol. 137, no. 3, p. 147, 1990, doi: 10.1049/ip-j.1990.0026.

[33] R. Hui, A. Mecozzi, A. D’Ottavi, and P. Spano, “Novel measurement technique of α factor in DFB semiconductor lasers by injection locking,” *Electron Lett*, vol. 26, no. 14, pp. 997–998, Jul. 1990, doi: 10.1049/el:19900647.

[34] H. Nakajima and J.-C. Bouley, “Observation of power dependent linewidth enhancement factor in 1.55 μm strained quantum well lasers,” *Electron Lett*, vol. 27, no. 20, pp. 1840–1841, Sep. 1991, doi: 10.1049/el:19911143.

[35] M. P. van Exter and J. P. Woerdman, “Determination of α factor of Fabry-Pérot-type semiconductor laser by injection locking,” *Electron Lett*, vol. 28, no. 17, pp. 1607–1608, Aug. 1992, doi: 10.1049/el:19921022.

[36] K. Iiyama, K. Hayashi, and Y. Ida, “Simple method for measuring the linewidth enhancement factor of semiconductor lasers by optical injection locking,” *Opt Lett*, vol. 17, no. 16, p. 1128, Aug. 1992, doi: 10.1364/OL.17.001128.

[37] H. BELLESCIZE, “La reception synchrone,” *Onde Electron*, vol. 11, pp. 230–240, 1932.

[38] K. R. Wendt and G. L. Fredendall, “Automatic Frequency and Phase Control of Synchronization in Television Receivers,” *Proceedings of the IRE*, vol. 31, no. 1, pp. 7–15, Jan. 1943, doi: 10.1109/JRPROC.1943.232382.

[39] J. Schrader, “A phase-lock receiver for the arraying of independently directed antennas,” *IEEE Trans Antennas Propag*, vol. 12, no. 2, pp. 155–161, Mar. 1964, doi: 10.1109/TAP.1964.1138181.

[40] G. R. VAUGHAN, E. F. OSBORNE, and G. S. ENTWISTOLE, “Locked oscillator phase modulator,” 1964.

[41] M. Peter and M. P. Strandberg, “Phase Stabilization of Microwave Oscillators,” *Proceedings of the IRE*, vol. 43, no. 7, pp. 869–873, 1955, doi: 10.1109/JRPROC.1955.278154.

[42] L. H. Enloe and J. L. Rodda, “Laser phase-locked loop,” *Proceedings of the IEEE*, vol. 53, no. 2, pp. 165–166, 1965, doi: 10.1109/PROC.1965.3585.

[43] W. R. Leeb, H. K. Philipp, A. L. Scholtz, and E. Bonek, “Frequency synchronization and phase locking of CO_2 lasers,” *Appl Phys Lett*, vol. 41, no. 7, pp. 592–594, Oct. 1982, doi: 10.1063/1.93620.

[44] J. SooHoo and C. L. Hayes, “Phase locking of a multimode to a single-mode He–Ne laser,” *Opt Lett*, vol. 4, no. 7, p. 202, Jul. 1979, doi: 10.1364/OL.4.000202.

[45] J. Hall, Ma Long-Sheng, and G. Kramer, “Principles of optical phaslavikse-locking: Application to internal mirror He-Ne lasers phase-locked via fast control of the discharge current,” *IEEE J Quantum Electron*, vol. 23, no. 4, pp. 427–437, Apr. 1987, doi: 10.1109/JQE.1987.1073354.

[46] L. G. Kazovsky and D. A. Atlas, “A 1320-nm experimental optical phase-locked loop: performance investigation and PSK homodyne experiments at 140 Mb/s and 2 Gb/s,” *Journal of Lightwave Technology*, vol. 8, no. 9, pp. 1414–1425, 1990, doi: 10.1109/50.59173.

[47] L. G. Kazovsky and D. A. Atlas, “A 1320 nm experimental optical phase-locked loop,” *IEEE Photonics Technology Letters*, vol. 1, no. 11, pp. 395–397, Nov. 1989, doi: 10.1109/68.43391.

[48] D. A. Atlas and L. G. Kazovsky, “2 Gbit/s PSK heterodyne communication system using optical phase-locked loop,” *Electron Lett*, vol. 26, no. 14, pp. 1030–1032, Jul. 1990, doi: 10.1049/el:19900668.

[49] L. Goldberg, R. D. Esman, and K. J. Williams, “Generation and control of microwave signals by optical techniques,” *IEE Proceedings J Optoelectronics*, vol. 139, no. 4, p. 288, 1992, doi: 10.1049/ip-j.1992.0049.

[50] R. C. Steele, “Optical phase-locked loop using semiconductor laser diodes,” *Electron Lett*, vol. 19, no. 2, pp. 69–71, Jan. 1983, doi: 10.1049/el:19830051.

[51] D. J. Malyon, D. W. Smith, and R. Wyatt, “Semiconductor laser homodyne optical phase-locked-loop,” *Electron Lett*, vol. 22, no. 8, pp. 421–422, Apr. 1986, doi: 10.1049/el:19860287.

[52] J. M. Kahn, “1 Gbit/s PSK homodyne transmission system using phase-locked semiconductor lasers,” *IEEE Photonics Technology Letters*, vol. 1, no. 10, pp. 340–342, Oct. 1989, doi: 10.1109/68.43368.

[53] J. Harrison and A. Mooradian, “Linewidth and offset frequency locking of external cavity GaAlAs lasers,” *IEEE J Quantum Electron*, vol. 25, no. 6, pp. 1152–1155, Jun. 1989, doi: 10.1109/3.29240.

[54] C.-H. Shin and M. Ohtsu, “Homodyne optical phase locking of resonant cavity coupled semiconductor lasers,” *IEEE J Quantum Electron*, vol. 29, no. 2, pp. 374–385, 1993, doi: 10.1109/3.199292.

[55] C.-H. Shin and M. Ohtsu, “Heterodyne optical phase-locked loop by confocal Fabry-Periot cavity coupled AlGaAs lasers,” *IEEE Photonics Technology Letters*, vol. 2, no. 4, pp. 297–300, Apr. 1990, doi: 10.1109/68.53268.

[56] H. R. Telle and H. Li, “Phase-locking of laser diodes,” *Electron Lett*, vol. 26, no. 13, pp. 858–859, Jun. 1990, doi: 10.1049/el:19900562.

[57] R. T. Ramos and A. J. Seeds, “Fast heterodyne optical phase-lock loop using double quantum well laser diodes,” *Electron Lett*, vol. 28, no. 1, pp. 82–83, Jan. 1992, doi: 10.1049/el:19920050.

[58] U. Gliese *et al.*, “A wideband heterodyne optical phase-locked loop for generation of 3-18 GHz microwave carriers,” *IEEE Photonics Technology Letters*, vol. 4, no. 8, pp. 936–938, Aug. 1992, doi: 10.1109/68.149915.

[59] G. Santarelli, A. Clairon, S. N. Lea, and G. M. Tino, “Heterodyne optical phase-locking of extended-cavity semiconductor lasers at 9 GHz,” *Opt Commun*, vol. 104, no. 4–6, pp. 339–344, Jan. 1994, doi: 10.1016/0030-4018(94)90567-3.

[60] E. Rubiola, Phase Noise and Frequency Stability in Oscillators. *Cambridge University Press*, 2008. doi: 10.1017/CBO9780511812798.

[61] Red Pitaya Hardware description [online]. Available at https://redpitaya.com/stemlab-125-14/

[62] R. Paschotta, “Noise in Laser Technology,” *Optik & Photonik*, vol. 4, no. 3, pp. 45–47, Oct. 2009, doi: 10.1002/opph.201190046.

[63] T. Okoshi, K. Kikuchi, and A. Nakayama, “Novel method for high resolution measurement of laser output spectrum,” *Electron Lett*, vol. 16, no. 16, pp. 630–631, Jul. 1980, doi: 10.1049/el:19800437.

[64] R. J. Baker, CMOS. *Wiley*, 2010. doi: 10.1002/9780470891179.

[65] D. W. Allan, “Should the classical variance be used as a basic measure in standards metrology?,” *IEEE Trans Instrum Meas*, vol. IM–36, no. 2, pp. 646–654, Jun. 1987, doi: 10.1109/TIM.1987.6312761.

[66] W. J. Riley, *NIST Special Publication 1065: Handbook of Frequency Stability Analysis*. Boulder, CO, USA: National Institute of Standards and Technology, 2008.

[67] D.-C. Shin, B. S. Kim, H. Jang, Y.-J. Kim, and S.-W. Kim, “Photonic comb-rooted synthesis of ultra-stable terahertz frequencies,” *Nat Commun*, vol. 14, no. 1, pp. 1–10, Feb. 2023, doi: 10.1038/s41467-023-36507-y.

[68] M. B. Marinov, B. Ganev, N. Djermanova and T. D. Tashev, "Analysis of Sensors Noise Performance Using Allan Deviation," *2019 IEEE XXVIII International Scientific Conference Electronics (ET)*, Sozopol, Bulgaria, 2019, pp. 1-4, doi: 10.1109/ET.2019.8878552.

[69] L.-S. Ma *et al.*, “Optical Frequency Synthesis and Comparison with Uncertainty at the 10^{-19} Level,” *Science (1979)*, vol. 303, no. 5665, pp. 1843–1845, Mar. 2004, doi: 10.1126/science.1095092.

[70] Th. Udem, R. Holzwarth, and T. W. Hänsch, “Optical frequency metrology,” *Nature*, vol. 416, no. 6877, pp. 233–237, Mar. 2002, doi: 10.1038/416233a.

[71] Jun Ye, H. Schnatz, and L. W. Hollberg, “Optical frequency combs: From frequency metrology to optical phase control,” *IEEE Journal of Selected Topics in Quantum Electronics*, vol. 9, no. 4, pp. 1041–1058, Jul. 2003, doi: 10.1109/JSTQE.2003.819109.

[72] S. A. Diddams, “The evolving optical frequency comb [Invited],” *Journal of the Optical Society of America B*, vol. 27, no. 11, p. B51, Nov. 2010, doi: 10.1364/JOSAB.27.000B51.

[73] V. Gerginov, C. E. Tanner, S. A. Diddams, A. Bartels, and L. Hollberg, “High-resolution spectroscopy with a femtosecond laser frequency comb,” *Opt Lett*, vol. 30, no. 13, p. 1734, Jul. 2005, doi: 10.1364/OL.30.001734.

[74] S. A. Diddams, L. Hollberg, and V. Mbele, “Molecular fingerprinting with the resolved modes of a femtosecond laser frequency comb,” *Nature*, vol. 445, no. 7128, pp. 627–630, Feb. 2007, doi: 10.1038/nature05524.

[75] I. Coddington, W. Swann, and N. Newbury, “Coherent Multiheterodyne Spectroscopy Using Stabilized Optical Frequency Combs,” *Phys Rev Lett*, vol. 100, no. 1, p. 013902, Jan. 2008, doi: 10.1103/PhysRevLett.100.013902.

[76] M. T. Murphy *et al.*, “High-precision wavelength calibration of astronomical spectrographs with laser frequency combs,” *Mon Not R Astron Soc*, vol. 380, no. 2, pp. 839–847, Sep. 2007, doi: 10.1111/j.1365-2966.2007.12147.x.

[77] H.-P. Doerr, T. Steinmetz, R. Holzwarth, T. Kentischer, and W. Schmidt, “A Laser Frequency Comb System for Absolute Calibration of the VTT Echelle Spectrograph,” *Sol Phys*, vol. 280, no. 2, pp. 663–670, Oct. 2012, doi: 10.1007/s11207-012-9960-5.

[78] D. J. Jones *et al.*, “Carrier-Envelope Phase Control of Femtosecond Mode-Locked Lasers and Direct Optical Frequency Synthesis,” *Science (1979)*, vol. 288, no. 5466, pp. 635–639, Apr. 2000, doi: 10.1126/science.288.5466.635.

[79] J. Ye *et al.*, “Accuracy Comparison of Absolute Optical Frequency Measurement between Harmonic-Generation Synthesis and a Frequency-Division Femtosecond Comb,” *Phys Rev Lett*, vol. 85, no. 18, pp. 3797–3800, Oct. 2000, doi: 10.1103/PhysRevLett.85.3797.

[80] A. C. Cardenas Olaya, S. Micalizio, M. Ortolano, C. E. Calosso, E. Rubiola, and J.-M. Friedt, “Digital electronics based on red pitaya platform for coherent fiber links,” in *2016 European Frequency and Time Forum (EFTF)*, IEEE, Apr. 2016, pp. 1–4. doi: 10.1109/EFTF.2016.7477826.

[81] A. Tourigny-Plante, V. Michaud-Belleau, N. Bourbeau Hébert, H. Bergeron, J. Genest, and J.-D. Deschênes, “An open and flexible digital phase-locked loop for optical metrology,” *Review of Scientific Instruments*, vol. 89, no. 9, pp. 1–5, Sep. 2018, doi: 10.1063/1.5039344.

[82] Z. Feng, A. Tourigny-Plante, J. Vojtěch, J. Genest, D. J. Richardson, and R. Slavík, “Comb-locked telecom-grade tunable laser using a low-cost FPGA-based lockbox,” in *Conference on Lasers and Electro-Optics*, Washington, D.C.: Optica Publishing Group, 2021, p. STu1J.4. doi: 10.1364/CLEO_SI.2021.STu1J.4.

[83] O. Lidoyne, P. Gallion, C. Chabran, and G. Debarge, “Locking range, phase noise and power spectrum of an injection-locked semiconductor laser,” *IEE Proceedings J Optoelectronics*, vol. 137, no. 3, p. 147, 1990, doi: 10.1049/ip-j.1990.0026.

[84] R. Hui, A. Mecozzi, A. D’Ottavi, and P. Spano, “Novel measurement technique of α factor in DFB semiconductor lasers by injection locking,” *Electron Lett*, vol. 26, no. 14, pp. 997–998, Jul. 1990, doi: 10.1049/el:19900647.

[85] T. Fortier and E. Baumann, “20 years of developments in optical frequency comb technology and applications,” *Commun Phys*, vol. 2, no. 1, pp. 1–16, Dec. 2019, doi: 10.1038/s42005-019-0249-y.

[86] V. Pacheco-Peña, “Terahertz Technologies and Its Applications,” *Electronics (Basel)*, vol. 10, no. 3, p. 268, Jan. 2021, doi: 10.3390/electronics10030268.

[87] G. Mouret *et al.*, “THz photomixing synthesizer based on a fiber frequency comb,” *Opt Express*, vol. 17, no. 24, p. 22031, Nov. 2009, doi: 10.1364/OE.17.022031.

[88] Y.-J. Kim, B. J. Chun, Y. Kim, S. Hyun, and S.-W. Kim, “Generation of optical frequencies out of the frequency comb of a femtosecond laser for DWDM telecommunication,” *Laser Phys Lett*, vol. 7, no. 7, pp. 522–527, Jun. 2010, doi: 10.1002/lapl.201010012.

[89] A. C. Cardenas Olaya, S. Micalizio, M. Ortolano, C. E. Calosso, E. Rubiola, and J.-M. Friedt, “Digital electronics based on red pitaya platform for coherent fiber links,” in *2016 European Frequency and Time Forum (EFTF)*, IEEE, Apr. 2016, pp. 1–4. doi: 10.1109/EFTF.2016.7477826.

[90] M. Matusko *et al.*, “Fully digital platform for local ultra-stable optical frequency distribution,” *Review of Scientific Instruments*, vol. 94, no. 3, pp. 1–7, Mar. 2023, doi: 10.1063/5.0138599.

[91] K. Balakier, L. Ponnampalam, M. J. Fice, C. C. Renaud, and A. J. Seeds, "Integrated Semiconductor Laser Optical Phase Lock Loops," *IEEE Journal of Selected Topics in Quantum Electronics*, vol. 24, no. 1, pp. 1–12, Jan. 2018, doi: 10.1109/JSTQE.2017.2711581.

[92] F. Wang *et al.*, "Simple, low-cost, and well-performing optical phase-locked loop for frequency and phase locking of semiconductor lasers," *Appl Opt*, vol. 62, no. 27, p. 7169, Sep. 2023, doi: 10.1364/AO.496663.

[93] S.-H. Yang and M. Jarrahi, "Navigating Terahertz Spectrum via Photomixing," *Opt Photonics News*, vol. 31, no. 7, p. 36, Jul. 2020, doi: 10.1364/OPN.31.7.000036.

[94] D.-C. Shin, B. S. Kim, H. Jang, Y.-J. Kim, and S.-W. Kim, "Photonic comb-rooted synthesis of ultra-stable terahertz frequencies," *Nat Commun*, vol. 14, no. 1, p. 790, Feb. 2023, doi: 10.1038/s41467-023-36507-y.

[95] A. R. Criado *et al.*, "Continuous-Wave Sub-THz Photonic Generation With Ultra-Narrow Linewidth, Ultra-High Resolution, Full Frequency Range Coverage and High Long-Term Frequency Stability," *IEEE Trans Terahertz Sci Technol*, vol. 3, no. 4, pp. 461–471, Jul. 2013, doi: 10.1109/TTHZ.2013.2260374.

[96] R. J. Steed *et al.*, "Hybrid Integrated Optical Phase-Lock Loops for Photonic Terahertz Sources," *IEEE Journal of Selected Topics in Quantum Electronics*, vol. 17, no. 1, pp. 210–217, Jan. 2011, doi: 10.1109/JSTQE.2010.2049003.

[97] G. Mouret *et al.*, "THz photomixing synthesizer based on a fiber frequency comb," *Opt Express*, vol. 17, no. 24, p. 22031, Nov. 2009, doi: 10.1364/OE.17.022031.

[98] T. Tetsumoto, F. Ayano, M. Yeo, J. Webber, T. Nagatsuma, and A. Rolland, "300 GHz wave generation based on a Kerr microresonator frequency comb stabilized to a low noise microwave reference," *Opt Lett*, vol. 45, no. 16, p. 4377, Aug. 2020, doi: 10.1364/OL.398345.

[99] T. Tetsumoto, T. Nagatsuma, M. E. Fermann, G. Navickaite, M. Geiselmann, and A. Rolland, "Optically referenced 300 GHz millimetre-wave oscillator," *Nat Photonics*, vol. 15, no. 7, pp. 516–522, Jul. 2021, doi: 10.1038/s41566-021-00790-2.

[100] J. R. Freeman *et al.*, "Injection locking of a terahertz quantum cascade laser to a telecommunications wavelength frequency comb," *Optica*, vol. 4, no. 9, p. 1059, Sep. 2017, doi: 10.1364/OPTICA.4.001059.

[101] M. Ravaro *et al.*, "Phase-locking of a 25 THz quantum cascade laser to a frequency comb using a GaAs photomixer," *Opt Lett*, vol. 36, no. 20, p. 3969, Oct. 2011, doi: 10.1364/OL.36.003969

[102] S. Barbieri *et al.*, "Phase-locking of a 2.7-THz quantum cascade laser to a mode-locked erbium-doped fibre laser," *Nat Photonics*, vol. 4, no. 9, pp. 636–640, Sep. 2010, doi: 10.1038/nphoton.2010.125.